Ingassing, Storage, and Outgassing of Terrestrial Carbon through Geologic Time

Rajdeep Dasgupta

Department of Earth Science
Rice University
6100 Main Street, MS 126
Houston, Texas 77005, U.S.A.

Rajdeep.Dasgupta@rice.edu

INTRODUCTION

Earth is unique among the terrestrial planets in our solar system in having a fluid envelope that fosters life. The secrets behind Earth's habitable climate are well-tuned cycles of carbon (C) and other volatiles. While on time-scales of ten to thousands of years the chemistry of fluids in the atmosphere, hydrosphere, and biosphere is dictated by fluxes of carbon between near surface reservoirs, over hundreds of millions to billions of years it is maintained by chemical interactions of carbon between Earth's interior, more specifically the mantle, and the exosphere (Berner 1999). This is because of the fact that the estimated total mass of C in the mantle is greater than that observed in the exosphere (Sleep and Zahnle 2001; Dasgupta and Hirschmann 2010) and the average residence time of carbon in the mantle is between 1 and 4 Ga (Sleep and Zahnle 2001; Dasgupta and Hirschmann 2006). But how did Earth's mantle attain and maintain the inventory of mantle carbon over geologic time? And is the residence time of carbon in the mantle, as constrained by the present-day fluxes, a true reflection of carbon ingassing and outgassing rates throughout Earth's history? Also, when in the planet's history did its mantle carbon inventory become established and how did it change through geologic time? The answers to these questions are important because of carbon's importance in a number of fields of Earth sciences, such as the thermal history of Earth [e.g., trace-volume carbonated melt may extract highly incompatible heat-producing elements from great depths (Dalou et al. 2009; Dasgupta et al. 2009b; Grassi et al. 2012)], the internal differentiation of the mantle and core [carbon influences element partitioning in both carbonate-silicate (e.g., Blundy and Dalton 2000; Dasgupta et al. 2009b; Dalou et al. 2009; Grassi et al. 2012) and metallic systems (Chabot et al. 2006; Hayden et al. 2011; Buono et al. submitted)], long-term evolution of climate (e.g., Kasting and Catling 2003; Hayes and Waldbauer 2006), and origin and evolution of life. Carbon also plays a role in the inner workings of the planetary mantle through mobilizing hydrogen from nominally anhydrous silicate minerals (Dasgupta et al. 2007a) and by stabilizing incipient carbonated melts in the mantle (e.g., Eggler 1976; Wyllie 1977; Dalton and Presnall 1998; Dasgupta and Hirschmann 2006; Dasgupta et al. 2013b). In the absence of carbon-induced melting and efficient extraction of such mobile melt, the presence of "water" in mineral structures controls the viscosity and the creep behavior of the mantle and determines whether a planet would "live" long (e.g., Earth), with systematic solid state convection that sustains plate tectonic cycles or "die" shortly after its birth (e.g., Mars and Venus), without a lasting tectonic cycle. Similarly, the presence of trace amounts of carbonated melt in Earth's upper mantle may be critical in regulating asthenospheric processes and stabilizing plate tectonics (Eggler 1976; Dasgupta et al. 2007a; Hirschmann 2010). Finally, any deep Earth carbon that is sequestered in the metallic core also influences the physical properties of inner and outer core (e.g., Poirier

1994; Hillgren et al. 2000; Mookherjee et al. 2011; Wood et al. 2013) and may have played a role in the dynamics of core formation, timing of core crystallization, and dynamics of magma ocean processes, including core-mantle segregation (Dasgupta et al. 2009a).

Because the abundance and mode of storage of mantle carbon are central to carbon's role in global geodynamics and controlling variables influencing carbon's distribution in other terrestrial reservoirs (crust plus atmosphere system and core), it is critical to constrain the processes that modulated the mantle carbon inventory through time. In this chapter, ingassing, outgassing, and storage mechanisms of terrestrial carbon, from the time period of early planetary differentiation and magma ocean in the Hadean Eon to the plate tectonic cycles of modern Earth through Phanerozoic, are reviewed (Fig. 1). Thus this chapter will primarily be in two parts: (1) inheritance of mantle carbon (focusing on Hadean processes) and (2) retention of mantle carbon (focusing on plate-tectonic cycling from Archean to present). The terms "ingassing" and "outgassing" are going to be used in a general sense, i.e., any mechanisms that introduce carbon to the mantle will be grouped as a carbon "ingassing" or acquisition mechanism and any mechanisms that remove carbon from the mantle will be listed as a carbon "outgassing" mechanism. The terms ingassing and outgassing are not used to imply that carbon is present in form of a gaseous phase.

CARBON INHERITANCE — MAGMA OCEAN CARBON CYCLE

How did Earth's mantle acquire or inherit its carbon budget and when did the inheritance take place? The origin of carbon on Earth, similar to many other volatile elements, is debated (Marty et al. 2013). The building blocks of Earth, which is traditionally thought to be carbonaceous chondrites, contain several weight percent of carbon depending on the sub-type (2.7-4.4 wt% with group average of 3.52 ± 0.48 wt%) (Anders and Grevesse 1989; Lodders 2003; Lodders 2010). Although carbonaceous chondrite is commonly used as the model for the terrestrial building block because of their compositional similarities with the solar photosphere (Lodders 2003), geochemical arguments for other types of chondrites and non-chondritic compositions, likely with quite different and lower abundance of carbon, also exist in modern literature (e.g., Alard et al. 2000; Javoy et al. 2010; Caro 2011; Warren 2011; Campbell and O'Neill 2012). Further, despite having concentration, in carbonaceous chondrite, on the order of weight percent, owing to very low condensation temperatures for carbon-bearing gases, ices, and other solid phases (e.g., CO, CH_4, and graphite; 41-626 K) carbon is thought to be largely lost during Earth's accretion (Abe 1997; Genda and Abe 2003). A similar decrease in the carbon abundance is also observed by comparing composition of solar photosphere to CI-type chondrites, where the latter incorporate only 10% of the photospheric carbon (Lodders 2003). Indeed, most of the estimates of bulk Earth carbon fall below 0.1 wt% (McDonough 2003; Marty 2012), although higher values (0.09-0.37 wt%) are also proposed in earlier literature (Trull et al. 1993). Despite the fact that this bulk Earth carbon budget and the timing as to when this amount was acquired remain highly uncertain it is not implausible, however, that Earth inherited this amount from chondritic materials during accretion (Morbidelli et al. 2012). Assuming that some finite concentration of carbon was inherited from the time of planetary accretion, in the following the possible fate of such carbon during early Earth differentiation—core formation and magma ocean processes is reviewed.

Magma ocean carbon cycle during core formation

A number of studies discussed the importance and various scenarios of carbon fractionation in a magma ocean (Kuramoto and Matsui 1996; Kuramoto 1997; Dasgupta and Walker 2008; Hirschmann and Dasgupta 2009; Dasgupta and Hirschmann 2010; Hirschmann 2012; Dasgupta et al. 2013a) (Fig. 1). This initial fractionation is important as it must have had an effect on Earth's early thermal and dynamical evolution, its geochemical differentiation, its path to an
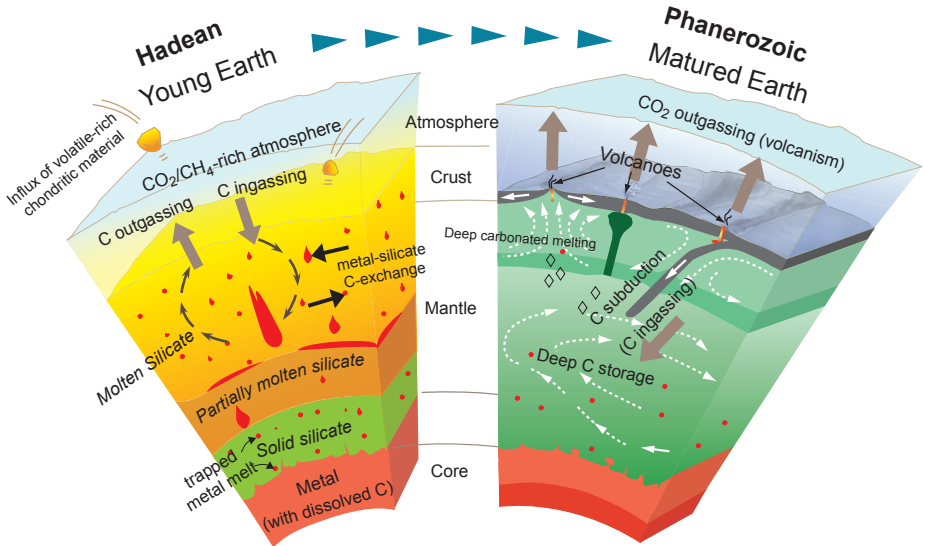
Figure 1. Cartoon illustrating the range of deep-Earth processes from magma ocean stage of the Hadean Eon to plate tectonic framework of the modern world that likely influenced the long-term carbon cycle. This chapter reviews Earth's deep carbon cycle in light of these processes. The early Earth processes cartoon (left), although shown together, may be temporally separated. For example, if carbon exchange between the proto-atmosphere and the magma ocean had an important role in the later evolution of the mantle, such a process was required to continue after the core formation had ceased (see text for details).

equable climate, and development of prebiotic chemistry. Magma ocean processes must have also set the initial distribution of carbon and conditions for further development of Earth's deep carbon cycle and have forced Earth to evolve differently compared to the planet Mars (Kuramoto 1997). The key information on the fate of carbon during early Earth differentiation is how the element was partitioned between various reservoirs, viz. core, mantle (magma ocean), and proto-atmosphere.

Equilibrium fractionation of carbon between the core and mantle and the contribution of core towards bulk Earth carbon inventory. Several studies over the last three decades have attempted to constrain the partitioning of siderophile elements between metallic and silicate melts in magma ocean environments, but similar experiments constraining volatile element fractionation remained limited (e.g., Li and Agee 1996; Okuchi 1997). Fractionation of elements, such as siderophile elements, between metallic core and silicate mantle during core formation was largely responsible for setting the elemental distribution in the terrestrial reservoirs and setting the stage for crust and mantle geochemistry to evolve. The same fractionation process likely also had influenced the bulk distribution of the terrestrial volatiles in general and carbon in particular (Kuramoto and Matsui 1996; Kuramoto 1997; Dasgupta and Walker 2008; Dasgupta et al. 2013a). If the entire bulk Earth carbon budget participated in the metal-silicate fractionation, and if $D_C^{metal/silicate}$ (partition coefficient of carbon between metal and silicate = mass fraction of carbon in metal melt/ mass fraction of carbon in silicate melt) is <1, then carbon would be concentrated mostly in the outer silicate layer. On the other hand, if $D_C^{metal/silicate} \gg 1$ then bulk carbon of the planet would mostly be sequestered into the core and hence would have much less impact on the long-term carbon cycle. If carbon really behaved as a highly siderophile element, a late volatile-rich veneer or other post-core segregation processes would likely be responsible for bringing carbon to the planet. Alternatively, in the event carbon

preferentially partitioned into the core-forming liquid, a less extreme iron affinity for carbon ($D_C^{metal/silicate}$ >1) might have allowed Earth's molten silicate to retain enough carbon in dissolved form to explain Earth's present-day carbon budget of the mantle. In order to answer these questions, the knowledge of $D_C^{metal/silicate}$, over the plausible range of depth-temperature-oxygen fugacity-melt compositions is necessary. However, studies investigating partitioning of carbon between metallic and silicate melt are scarce (Dasgupta and Walker 2008; Dasgupta et al. 2012; Dasgupta et al. 2013a).

In the absence of any experimental measurements of $D_C^{metal/silicate}$, Dasgupta and Walker (2008) bracketed the possible range of $D_C^{metal/silicate}$ assuming that (1) the present-day inventory of mantle carbon (30-1100 ppm C), as derived from the concentration of the same in mantle derived magmas, was produced by equilibrium partitioning of carbon between metallic and silicate melt in a magma ocean, (2) the entire present-day core mass of 32.3% equilibrated with the whole mantle melt of 67.7%, and (3) a maximum of ~6-7 wt% C can be dissolved into the metallic melt at magma ocean conditions. This analysis suggested that with bulk Earth carbon of 730 ppm (McDonough 2003), the bulk core will end up acquiring 0.25 ± 0.15 wt% C. If more recent bulk Earth carbon estimate of 530 ± 210 ppm (Marty 2012) is used, the core carbon estimate would be slightly lower. However, it is important to note that Marty's (2012) bulk Earth carbon estimate assumes that there is no carbon in the core and distributes the bulk silicate Earth (BSE) carbon content to the whole Earth mass (5.98×10^{27} g). But the mass balance calculation of Dasgupta and Walker (2008) showed that Earth's core can store as much as ($4.8 \pm 2.9) \times 10^{24}$ g C, i.e., the metallic core alone can contribute as much as 803 ppm C to bulk Earth. The analysis of Dasgupta and Walker (2008), although simple, highlighted the importance of possible carbon storage in the core towards the total inventory of bulk Earth carbon.

More recent experimental effort generated direct measurements of $D_C^{metal/silicate}$ at shallow magma ocean conditions (Dasgupta et al. 2012; Dasgupta et al. 2013a). These experiments at 1-5 GPa and 1500-2100 °C at oxygen fugacity (f_{O_2}) 1.5 to 2 log units below the iron-wüstite buffer (~IW−1.5 to IW−2.0) explored carbon partitioning between Fe-rich metallic melt and mafic-ultramafic silicate melts (non-bridging oxygen over tetrahedrally coordinated cations, NBO/T of 0.9-2.8). These studies demonstrated that carbon indeed behaves as a strongly siderophile element ($D_C^{metal/silicate}$ varying between ~5500 and >150) and metal affinity of carbon increases with increasing pressure and decreases with increasing temperature, silicate melt depolymerization, extent of hydration, and oxygen fugacity. Despite these experimental measurements, more work needs to be done to fully explore the effect of various key intensive variables on $D_C^{metal/silicate}$. In particular, experiments will need to quantify $D_C^{metal/silicate}$ relevant for magma oceans that are quite deep (Li and Agee 1996; Chabot and Agee 2003; Righter 2011) and more reduced (Wood et al. 2006). As pointed out by Dasgupta et al. (2013a), future experiments will also have to take into account more complex metallic alloy liquid chemistry including the presence of sulfur, silicon, and oxygen and a known fugacity of other trace gases such as H_2O and H_2 that can influence the speciation of carbon in silicate melts. But because the conditions of core-mantle equilibration continue to be a subject of active debate (e.g., Righter 2011; Rubie et al. 2011), it is worth exploring the predictions based on already constrained values of $D_C^{metal/silicate}$ on the relative carbon budget of core and the mantle.

Figure 2, modified from Dasgupta et al. (2013a), shows the predicted concentration of carbon in the core and the BSE as a function of bulk Earth carbon that participated in the core-mantle fractionation in a magma ocean. For this calculation, it was assumed that the present-day mass of Earth's core (32.3% by weight of Earth) equilibrated with the whole molten mantle, i.e., the concentration of carbon in the core, C_C^{core} and the concentration of carbon in the mantle, C_C^{mantle} are related to the bulk Earth carbon, C_C^0 and $D_C^{metal/silicate}$ by the following equations:
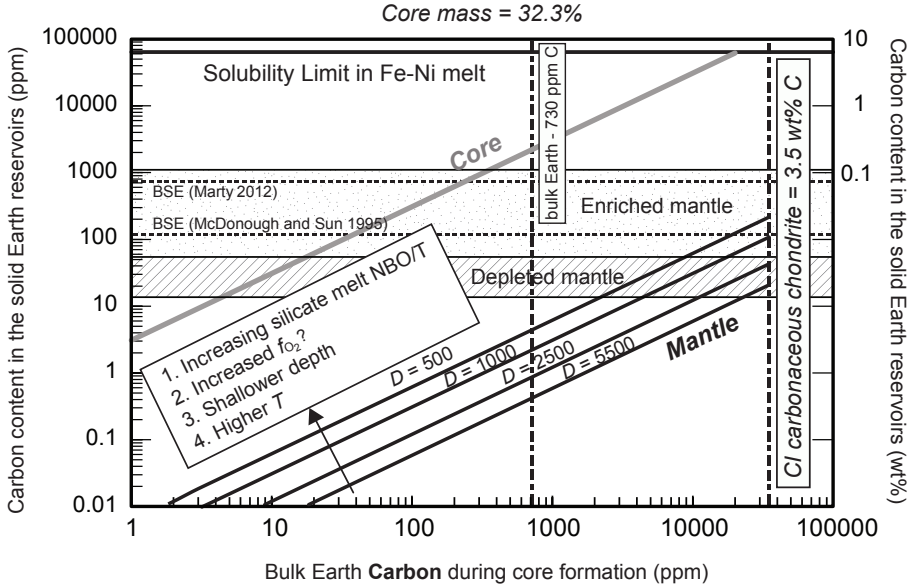
Figure 2. The effect of equilibrium partitioning of carbon between metallic and silicate melt in a magma ocean on the inventory of mantle and core carbon, modified after Dasgupta et al. (2013a). This calculation assumes that the inventory of carbon in the BSE and the core reflects perfect equilibration of the present-day mass of the core (32.3%) with the mass of silicate Earth. Carbon concentration of deep Earth reservoirs (core: grey curve and mantle: black curves) are plotted as a function of bulk Earth carbon that participated in the core-mantle fractionation event. The mantle and core concentrations are plotted for four different $D_C^{metal/silicate}$ values of 5500, 2500, 1000, and 500, which may cover all the possible conditions of core-mantle equilibration. The higher values are appropriate for magma ocean that is deep, dry, and more reduced. Plotted for comparison are the estimated range of modern Earth mantle carbon contents [depleted mantle similar to the source regions of mid-ocean ridge basalts: ~50-200 ppm CO_2 (Marty and Tolstikhin 1998; Saal et al. 2002; Cartigny et al. 2008); enriched mantle similar to the source regions of intraplate ocean island basalt or off-axis seamounts: up to 4000 ppm CO_2; (Pineau et al. 2004)], primarily based on volcanic CO_2 flux and the estimate of BSE carbon content of 120 ppm (McDonough and Sun 1995) and ~765 ppm (Marty 2012). Also plotted for reference are the carbon abundance in CI chondrite of ~3.5 wt% (Anders and Grevesse 1989; Lodders 2003), estimated bulk Earth carbon content of 730 ppm (McDonough 2003), and carbon solubility limit for Fe-rich alloy melt at high temperature and low pressure (Dasgupta and Walker 2008; Nakajima et al. 2009; Siebert et al. 2011; Dasgupta et al. 2013a).

$$C_C^{core} = \frac{C_C^0 - 0.677C_C^{mantle}}{0.323} \qquad (1)$$

$$C_C^{mantle} = \frac{C_C^0}{0.323 D_C^{metal/silicate} + 0.677} \qquad (2)$$

Given that magma ocean metal-silicate equilibration likely took place over a range of P-T-f_{O_2} (Wood et al. 2006), in Figure 2 the estimated carbon content of the core and the mantle residual to core formation are plotted for $D_C^{metal/silicate}$ varying from 5500 to 500. The higher $D_C^{metal/silicate}$ values likely capture carbon fractionation in a very deep magma ocean under more reduced conditions, with very dry magma ocean (low fugacity of H_2 and H_2O), or for evolved silicate magma compositions and the lower $D_C^{metal/silicate}$ values capture carbon fractionation scenarios in shallower or wet magma oceans, with extreme temperatures, and more primitive (higher degree of melt depolymerization) compositions.
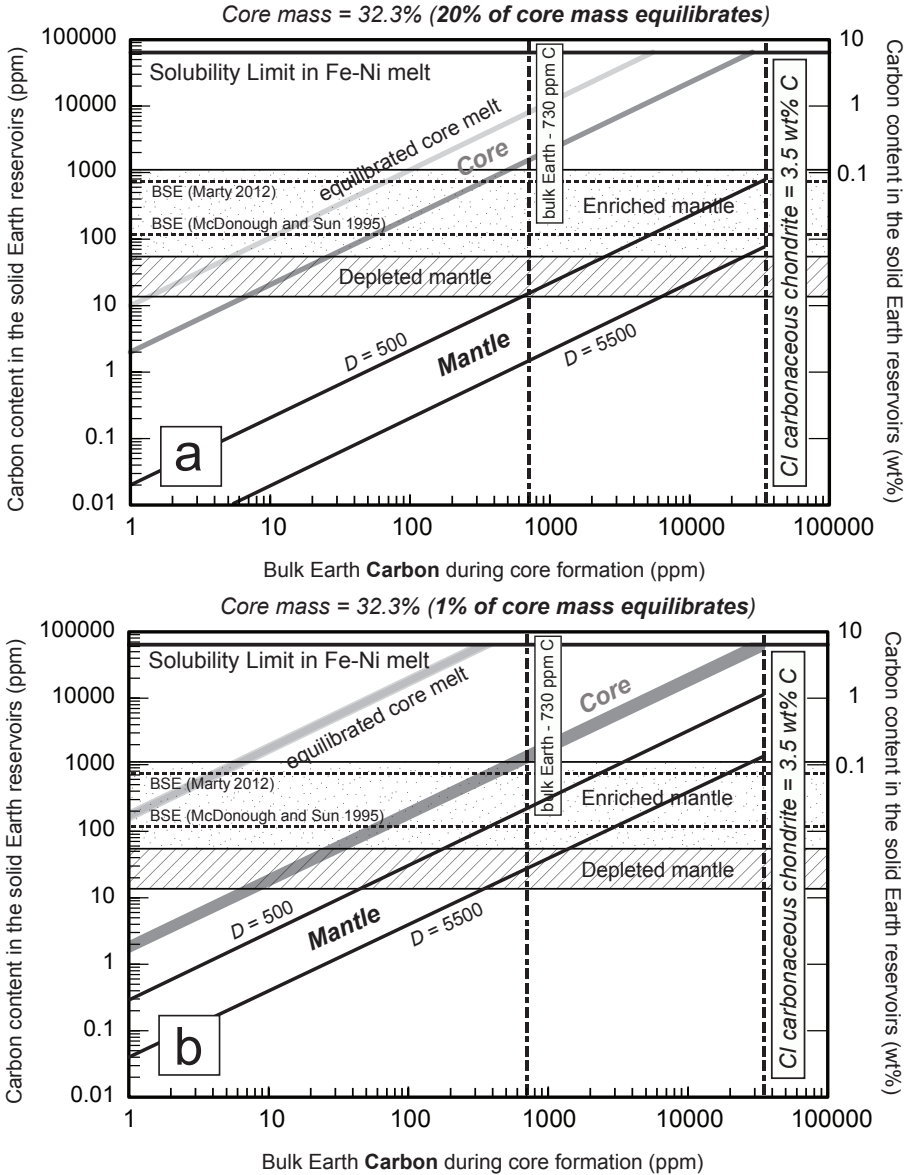
Figure 2 adopted from Dasgupta et al. (2013a) suggests that the average carbon content of Earth's present-day depleted mantle can be matched by equilibrium core-mantle fractionation of carbon if bulk Earth carbon during core formation was ≥0.4-3.5 wt% (≥4000-35000 ppm C). In order to generate enriched mantle domains similar to those of some of the ocean island basalt (OIB) source regions (50-1000 ppm C in the source), a minimum bulk Earth carbon of 2.1 wt% and in excess of 3.5 wt% is necessary. The abundance of bulk Earth carbon during core-mantle segregation is uncertain, however. Many estimates of bulk Earth carbon suggest values ≤1000 ppm (McDonough 2003; Marty 2012). Owing to volatility of carbon during the accretion process, carbon is thought to be largely lost from the chondritic building blocks. If the available bulk Earth carbon was only ~730 ppm (McDonough, 2003), for the plotted range of $D_C^{metal/silicate}$, the molten mantle residual to core formation could only possess 0.4-4.5 ppm C (1.5-16.5 ppm CO_2). This value is only 3-33% of the present-day mantle budget of carbon with 50 ppm bulk CO_2 (~14 ppm C). If the modern bulk mantle C content is closer to the carbon for enriched mantle domains (e.g., 500 ppm CO_2 or 136 ppm C), the contribution of carbon that was left behind after core formation will be even smaller. In this latter case or if the primitive mantle C content estimate of 120 ppm, after McDonough and Sun (1995), is used, the equilibrium core formation will leave behind a molten silicate that contains only 0.3-3.8% of the present-day mantle carbon. If the BSE carbon content of ~765 ppm (Marty 2012) is used then >99% of silicate Earth C needs to be derived from post core-segregation processes. Hence, whatever the exact carbon content of the present-day BSE is, such concentration is in excess with respect to what is predicted by magma ocean chemical equilibration.

The analysis presented above clearly suggests that, owing to siderophile nature of carbon in core-forming magma ocean conditions, only a small fraction of the present-day mantle or BSE carbon can be primordial, which dates back to the Hadean Eon prior to the last giant impact. In other words, most of the primordial carbon, which dates back prior to core formation time and not degassed to atmosphere or lost to space, was likely sequestered into the metallic core. The measured range of $D_C^{metal/silicate}$ and bulk Earth carbon of 730 ppm (McDonough, 2003) make the bulk core store ~0.23 wt% C. This concentration of carbon in the bulk core (1.932×10^{27} g) makes a total of 4.44×10^{24} g C, or ~744 ppm C for the whole Earth. This calculation underscores the importance of knowing the carbon abundance that participated in the core-formation processes, because with core contribution of >700 ppm C for bulk Earth, the estimate of bulk Earth carbon can at least double. For example, if the estimate of BSE carbon content of 765 ± 300 ppm C is normalized with respect to the whole Earth, a bulk Earth carbon content of 530 ± 210 ppm C results (Marty 2012). But with 0.23 wt% carbon in the core, the bulk Earth carbon content becomes as much as 1277 ± 210 ppm C. The estimate of 0.23 wt% C in the core derived from experimental partition coefficients of carbon between metallic and silicate melt (Dasgupta et al. 2013a) is similar to the earlier estimates obtained based on mass balance approach (McDonough 2003; Dasgupta and Walker 2008). The value of ~0.2 wt% carbon in the core is also consistent with the Pb-isotopic age of Earth, which seems to require strong partitioning of Pb into the core throughout Earth's accretion and Pb behaves as a strongly siderophile element only when the carbon content of the metallic liquid is small and far from saturation (Wood and Halliday 2010). However, although these geochemical estimates are all converging towards only a modest carbon content of the bulk core, some earlier work suggested carbon core content as much as 1.2 wt% (Yi et al. 2000). The work of Wood et al. (2013) estimated a similar but somewhat higher abundance of carbon in the core than those derived from currently available partitioning data. These authors (Wood et al. 2013) suggested, based on the C/S ratio of accreting materials and the effect of S on siderophile element partitioning between metal and silicate, that the core contains ~0.6 wt% carbon.

With the metallic core taking possession of Earth's carbon during the Hadean eon, an explanation of the modern mantle carbon budget requires some later replenishment event. This is the essence of the "excess" mantle carbon paradox. If perfect core-mantle equilibration

is conceived, then the only way to avoid this is for bulk Earth to have as much carbon as carbonaceous chondrite (Fig. 2). However, even if there was 3.5 wt% carbon taking part in core-mantle fractionation, the residual silicate liquid would not retain enough carbon to match the BSE estimate of 765 ± 300 ppm C as proposed by Marty (2012). Also, with as much as 3.5 wt% C available, carbon could end up being the sole light element in the core, reaching the Fe-rich melt saturation value of ~8-10 wt% (Dasgupta and Walker 2008; Lord et al. 2009; Nakajima et al. 2009; Siebert et al. 2011; Dasgupta et al. 2013a) and perhaps precipitating graphite or diamond in the mantle. But given the low condensation temperatures of relevant carbon compounds, it is extremely unlikely that weight percent level carbon was acquired from chondritic building blocks. With the magma ocean being depleted in carbon instantly after core segregation, other processes to bring back carbon to the present-day BSE budget need to be invoked. What can some of those processes be?

Heterogeneous accretion and imperfect metal-silicate equilibration during core formation: the fate of carbon. If the dynamics of core-mantle separation are considered in detail, the possibility of perfect equilibration between metallic and silicate melt in a magma ocean occurs when the core melt is thoroughly emulsified in the magma ocean. In other words, sinking metal melt droplets had to have the dimensions smaller than the length scale of diffusive equilibration for elements of interest. Metal droplet diameters of ~1 cm is thought to be required for efficient equilibration with silicate melts. This likely happened when undifferentiated objects accreted or when small impactors (differentiated or undifferentiated) collided with proto-Earth, setting the equilibrium fractionation of carbon and other siderophile elements. But the geochemistry of Hf-W isotope systematics (Halliday 2004) and also those of Ni, Co, and W (Rubie et al. 2011) seem to require imperfect equilibration. Dahl and Stevenson (2010) showed that if the dynamics of accretion of large, differentiated impactors are considered, it is possible to have scenarios where the core of the giant impactor merges directly with the proto-Earth core, bypassing major chemical interaction with Earth's mantle. If this was the case, then the core:mantle mass ratio relevant for equilibrium partitioning of carbon (and any other elements) could be very different than their relative present-day masses. Dahl and Stevenson (2010) argued that only 1-20% of the cumulative core mass might have equilibrated with the magma ocean when late, differentiated, large impactors collided with proto-Earth. In this specific case, one could envision the most extreme cases of core to mantle masses (~1:210 to 1:10.5) relevant for equilibration. Dasgupta et al. (2013a) showed that with such mass ratios and for a bulk Earth carbon of 730 ppm, the magma ocean could retain as much as ~1.5 (20% of core mass equilibrating with the magma ocean and with $D_C^{metal/silicate}$ of 5500) to 217 ppm (1% of cumulative core mass equilibrating with the magma ocean with $D_C^{metal/silicate}$ of 500) carbon in dissolved form (Fig. 2). Interestingly, in the latter case, i.e., if only 1-2% of the metallic core mass equilibrated with the entire magma ocean, mass balance predicts core liquid to dissolve 10-15 wt% C. But such concentration could be higher than the solubility of carbon alloy in liquid at magma ocean conditions (Fig. 3; (Dasgupta and Walker 2008; Nakajima et al. 2009; Siebert et al. 2011; Dasgupta et al. 2013a). Thus the most extreme form of core-mantle disequilibrium—a very small fraction of alloy liquid equilibrating with a large mass of molten silicate—could have forced over-saturation of graphite or diamond during core segregation. In this scenario, the diamond or graphite would float from the segregating core liquid and contribute to the overlying silicate magma ocean carbon budget. Thus one might argue that this extremely imperfect core-mantle equilibration scenario could eliminate the "excess carbon" in the mantle problem by letting the magma ocean possess sizeable carbon content in solution and by forcing the segregating alloy liquid leave behind graphite or diamond. This model is similar to the one proposed by Hirschmann (2012). It should be noted that the carbon content of Earth's core becomes quite uncertain in this scenario, because the final make-up of the core depends on the composition and relative masses of the cores of different impactors. Dasgupta et al. (2013a) argued this scenario may be unlikely; because when the core of a large impactor merges directly

Figure 3. The effect of incomplete alloy melt-silicate melt equilibrium on the inventory of mantle and core carbon. The calculation in this figure assumes that between 20% (a) and 1% (b) of the present-day core mass equilibrated with the silicate magma ocean. The fraction of metallic alloy melt mass that equilibrated with the mantle was taken from Dahl and Stevenson (2010), who specifically modeled the impact of an already differentiated object with the proto-Earth, for the case where very limited metal-silicate equilibration takes place before the core of the impactor merges with the core of the proto-Earth. Shown for reference from Figure 2 are the present day mantle carbon content estimates for depleted and enriched sources, the BSE carbon content estimates, bulk Earth carbon content estimate of McDonough (2003), and carbon content of CI-type meteorite. For the sake of clarity, calculations are shown for only two $D_{\mathrm{C}}^{metal/silicate}$ values of 500 and 5500. In general, if only a small fraction of the segregating alloy liquid equilibrates with the magma

with the core of proto-Earth, the latter fractions of accreting metallic melt may not equilibrate with the entire silicate mantle mass. In particular, the other side of the planet and/ or the lower part of the solid mantle, would not provide storage for carbon (Keppler et al. 2003; Shcheka et al. 2006). Unmolten silicates will also not allow extreme metallic to silicate melt mass ratio for chemical equilibration (Golabek et al. 2008) necessary to force metallic liquid into carbon saturation. Hence, even if most of the terrestrial volatiles, including carbon, were delivered to Earth during the late stage of magma ocean and accretion (Morbidelli et al. 2012), it is unclear whether the very low ratio of alloy: silicate melt necessary for carbon saturation of segregating alloy liquid was ever achieved. Moreover, it has been argued that thorough emulsification of differentiated impactors' cores is achieved (conditions required for equilibrium separation of the core and the mantle) when dynamics of the impact process are considered (Kendall and Melosh 2012). Finally, even if thorough emulsification of the cores of large impactors did not take place the terrestrial magma ocean, metal-silicate equilibration with respect to carbon might have still taken place. Dasgupta et al. (2013a) pointed out that the length scale of diffusion for carbon in alloy melt is longer than that for common siderophile elements (Goldberg and Belton 1974; Dobson and Wiedenbeck 2002). Hence, if some modest fraction of carbon was available during the main stage of accretion and alloy-magma ocean equilibration, carbon partitioning in a system with alloy:silicate melt ratio not too different from the respective present-day masses mantle and core likely took place.

Magma ocean carbon cycle after core formation

Magma ocean storage capacity of carbon. Although the above analysis shows that the bulk of the carbon available in magma ocean environment during core formation was likely partitioned into the core, it also suggests the ability of silicate magma to keep in solution some finite fraction of carbon. This observation is unlike some previous suggestions where carbon was thought to be perfectly incompatible in silicate magma during core-mantle equilibration (Kuramoto and Matsui 1996; Kuramoto 1997; Yi et al. 2000). Given the uncertainty in bulk Earth carbon in general and the concentration prevalent during the Hadean time in particular, it is important to evaluate the storage capacity of carbon of the terrestrial magma ocean so that the limit to which magma ocean could supply carbon to the crystallizing mantle can be evaluated. The knowledge of magma ocean storage capacity of carbon is also important so that the conditions of appearance of various carbon-rich accessory phases (e.g., graphite/diamond, Fe-carbide, silicon carbide, C-rich alloy melt/ sulfide-rich melt with dissolved carbon, carbonated melt, and crystalline carbonate) can be constrained as a function of evolving temperature and oxygen fugacity of the planet.

The storage capacity of carbon in silicate liquid depends strongly on the dominant speciation or bonding environment of carbon, which in turn is controlled by a number of key variables including pressure, temperature, melt composition, and the last but not the least, the fugacity of oxygen, f_{O_2} and fugacity of other volatile species, such as f_{H_2O} and f_{H_2} that may impact carbon dissolution (Hirschmann 2012; Dasgupta et al. 2013a). Based on the spectroscopic studies of natural and experimental glasses at the conditions relevant for the basalt genesis of modern

---

(*continuation of Figure 3 caption*)
ocean, the latter is more likely to retain a good fraction of Earth's bulk carbon. It can be noted that with bulk Earth carbon of 730 ppm, the magma ocean can achieve as much as 27-217 ppm C (b), which overlaps with the estimates of present-day mantle budget. Also, in this case the equilibrating fraction of alloy melt may reach C-saturation (~8 wt% C) and hence release graphite/diamond. Flotation of these diamonds may elevate the magma ocean C-content thus perhaps even attaining the BSE value of ~765 ppm C (Marty 2012). However, it is argued in the text that this extreme case of incomplete core-mantle equilibration is unlikely. The bulk core carbon content estimation (dark grey lines) assumes that the unequilibrated fraction of the segregating metallic melt contained no carbon.

Earth, carbon is known to dissolve in mafic-ultramafic melts chiefly as carbonate anions bonded to network modifiers such as Ca^{2+}, Mg^{2+}, and Fe^{2+} (Blank and Brooker 1994; Dixon 1997; Brooker et al. 2001; Morizet et al. 2002; Lesne et al. 2011). However, CO_2 solubility in silicate liquids decreases with decreasing oxygen fugacity (Pawley et al. 1992; Thibault and Holloway 1994; Morizet et al. 2010; Mysen et al. 2011) and at conditions as reduced as Fe-metal saturation (~IW), carbonates may not be the dominant carbon species of interest for reduced magma oceans. Thus Equilibria of C-O-H fluids as a function of oxygen fugacity suggest that at f_{O_2} at or near core-forming conditions (IW−4 to IW+1), the dominant fluid species of interest are CH_4, CO, and H_2 rather than CO_2 and H_2O (e.g., Holloway and Jakobsson 1986; Zhang and Duan 2009). Although the number of studies investigating the solubility and dissolution of carbon in silicate melt at similarly reduced conditions are scarce, the available studies suggest that CO, CH_4 (or other higher order C-H molecules or groups, such as alkyne group (C≡C-H) bonded to silicate network), metal carbonyl groups, and possible structural units such as Si-C (Kadik et al. 2004; Kadik et al. 2006; Mysen and Yamashita 2010; Mysen et al. 2011; Wetzel et al. 2012; Dasgupta et al. 2013a) are all important species to be considered for carbon in reduced melts. Therefore, the topic of interest is the storage capacity of carbon species at reduced magma ocean conditions.

Figure 4 compiles the available experimental data of carbon solubility in silicate melts at conditions reduced enough to be relevant for core-mantle equilibration (IW−1 to IW−4;
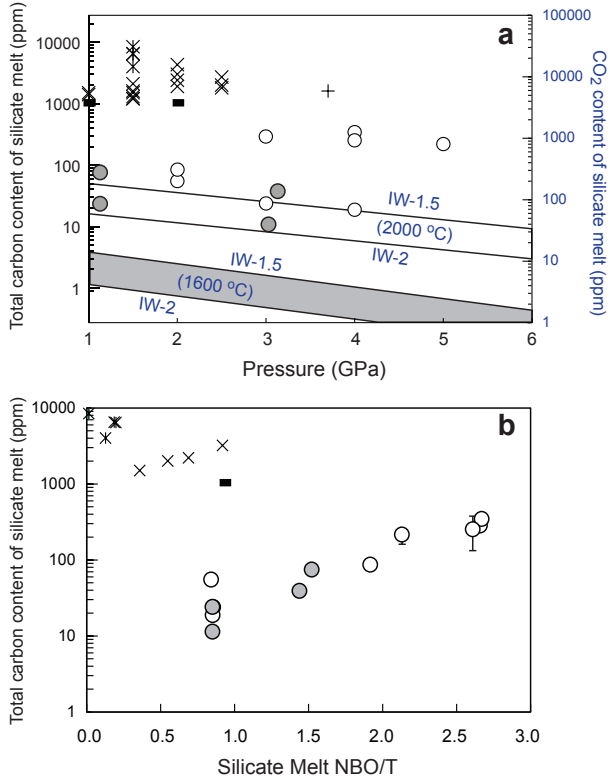
Reference	$\log f_{O_2}$ (ΔIW)	T (°C)
■ Holloway and Jakobsson (1986)	0	1200
+ Kadik et al. (2004)	-2.3	1520-1600
✕ Mysen et al. (2009)	0	1400
✻ Kadik et al. (2011)	-1.9 to -3.7	1400
◐ Dasgupta et al. (2013a)	-1.5 to -2.0	1600-2000

Figure 4a,b. Storage capacity of carbon in silicate magma at core-forming conditions (f_{O_2} ~IW−4 to IW). modified after Dasgupta et al. (2013a). (a) Total carbon content in silicate melts as a function of pressure. A range of silicate compositions saturated with CH_4-H_2 fluid and/or graphite and at temperatures of 1200-2000 °C is plotted. Also shown for reference are the CO_2 solubilities in a tholeiitic basalt at graphite saturation at 1600 and 2000 °C and between f_{O_2} similar to IW−2 to IW−1.5, following the model of Holloway (1992). (b) Estimated concentration of total dissolved carbon in silicate melt as a function of melt depolymerization index NBO/T (Mysen 1991) for the studies plotted in (a).

Wood et al. 2006) or early stages of cooling magma ocean, soon after core formation (up to IW+1). Both C-rich vapor saturated (Holloway and Jakobsson 1986; Jakobsson and Holloway 1986; Mysen et al. 2009) and vapor-absent, graphite-saturated (Kadik et al. 2004; Kadik et al. 2011; Dasgupta et al. 2012, 2013a) experiments are included. The key features of dissolved carbon content in basaltic silicate melt (mostly at graphite saturation) are its increase with increasing temperature and melt depolymerization index as expressed by NBO/T, and decrease with increasing pressure. The dependence of total carbon solubility on pressure and temperature mimics what is expected for $CO_2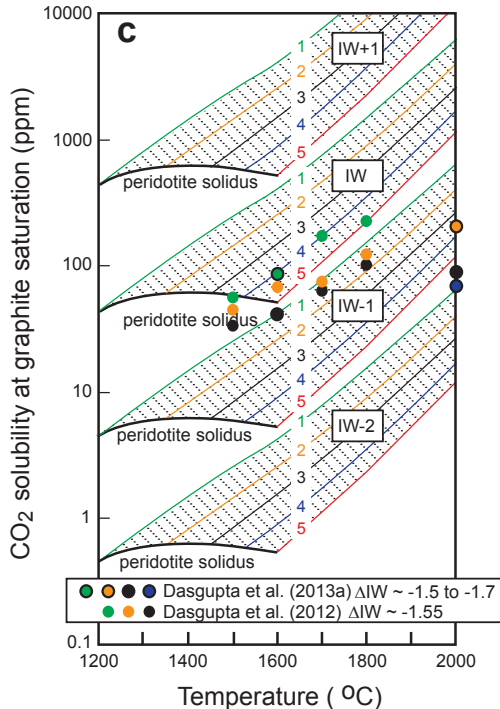$ solubility at graphite saturation (Holloway et al. 1992; Hirschmann and Withers 2008) (Fig. 4c). However, the total carbon content in tholeiites, at a $f_{O_2} <$ IW, remains as much as an order of magnitude higher than the value expected for carbon dissolved only as carbonates (Dasgupta et al. 2013a). If total dissolved carbon content in tholeiitic melt saturated with CH_4-H_2 fluid reported by Holloway and Jakobsson (1986) is appropriate (Fig. 4a,b), then the contribution of the reduced or hydrogenated species to the total carbon content may be even higher. Furthermore, when CO_2 solubility predictions of reduced, graphite-saturated melts are compared with total dissolved carbon content at graphite saturation in more depolymerized (peridotitic, komatiitic) melts (Dasgupta et al. 2013a), it is observed that the difference between the two are even more dramatic (Fig. 4a); i.e., the depolymerized melts may have up to three orders of magnitude higher carbon content than that expected from CO_2 solubility alone. This latter discrepancy may owe in part to the fact that the model of Holloway et al. (1992) was developed for a tholeiitic basalt and hence does not apply to more MgO-rich and depolymerized melt compositions. Indeed the total carbon contents at graphite saturation, obtained for tholeiitic compositions, are consistently lower compared to the ones for peridotitic, komatiitic, and alkali basaltic compositions in the study of Dasgupta et al. (2013a). This observation suggests that the carbon solubility at graphite saturation is higher for more depolymerized melts (Fig. 4a) and thus the lat-

Figure 4c. Storage capacity of carbon in silicate magma at or near core-forming conditions (f_{O_2} ~IW−2 to IW+1). (c) CO_2 solubility in a tholeiitic basalt at graphite saturation as a function of temperature at 1-5 GPa and reduced conditions compared to the total dissolved carbon measured in a number of studies on tholeiitic compositions (Dasgupta et al. 2012; Dasgupta et al. 2013a) at similarly reducing conditions. The data and calculated lines are color-coded by pressure - 1 GPa - green, 2 GPa - orange, 3 GPa - black, 4 GPa - blue, and 5 GPa - red. This plot shows that the total carbon content at graphite saturation for tholeiitic basalts increases with increasing temperature and decreases with increasing pressure and these systematics are similar to what is expected for CO_2 solubility from thermodynamic calculations. However, the experimentally measured total dissolved carbon content at a given oxygen fugacity is significantly higher than that of the carbon in the form of dissolved carbonates alone, which highlights the role of other reduced species and f_{H_2} and f_{H_2O} in the magma ocean storage capacity of carbon.

ter are more appropriate for magma ocean carbon saturation limits. More work in calibrating the CO_2 solubility in Fe-Mg-rich depolymerized basalts at graphite saturation and at reduced (IW−2 to IW+1) conditions will be needed to evaluate what fraction of the total dissolved carbon in the terrestrial magma ocean was carbonated species and what fraction was metal carbonyl complexes and hydrogenated species, such as methane. Also, CO_2 storage capacity of mafic-ultramafic melts increases with f_{O_2} and f_{H_2O} (Eggler and Rosenhauer 1978; Holloway et al. 1992; Dasgupta et al. 2013a), so it is also going to be important to constrain the relative proportion of carbonated versus hydrogenated and other reduced species as a function of changing f_{O_2} of the magma ocean.

Magma ocean-atmosphere interaction and ingassing of carbon? The pressure and temperature dependence of storage capacity of carbon (either as CO_2 or as total dissolved carbon) at graphite saturation for the reduced magma ocean has important implications for the nature of interaction between magma ocean and proto atmosphere and for the fate of carbon during the crystallization of magma ocean.

A plausible mechanism for the BSE gaining carbon after core formation is through interaction of the magma ocean with the Hadean atmosphere (Hirschmann 2012; Dasgupta et al. 2013a). The negative effect of pressure on total carbon/CO_2 solubility at graphite saturation, as shown in the preceding section, makes this process viable. The depth dependence of CO_2 and total carbon solubility in mafic magma at graphite saturation and near iron-wüstite buffer (Fig. 4c) (Holloway et al. 1992; Hirschmann and Withers 2008; Dasgupta et al. 2013a) suggests that the carbon storage capacity of magma ocean at shallow depths is greater and diminishes at the expense of graphite/diamond or carbide-rich metallic melt at greater depths. In this scenario, a magma ocean could dissolve carbon through interaction with an early C-rich atmosphere and precipitate diamond/metal carbide melt in its deeper parts as convection brought a batch of magma down to greater depths. Precipitation and sequestration of carbon-rich phases at depth would lead to C-depletion of magma and thus upon upwelling would be able to dissolve more carbon/CO_2 from the atmosphere (Fig. 5b). This cycling might have served as an efficient mechanism of magma ocean ingassing, bringing the mantle inventory of carbon up to the present-day value or to match the suggested value of BSE well before magma ocean crystallization (Hirschmann 2012; Dasgupta et al. 2013a). The time scale over which this carbon ingassing process likely took place is unclear at present. The chemical evolution of Earth's primitive atmosphere is controversial (e.g., Kasting 1993; Zahnle et al. 2007; Zahnle et al. 2010) but several authors suggest persistence of a CO_2-rich atmosphere either through degassing of an earlier magma ocean (Elkins-Tanton 2008) or via condensation of a liquid water ocean, which could allow the residual atmosphere to be composed chiefly of CO_2 (Zahnle et al. 2007). CO_2-rich atmosphere could have existed when redox state of the shallow magma ocean was somewhat more oxidized than that imposed by saturation of metallic core liquid, i.e., when dissolved C-species in magma at shallow depths was dominantly CO_2 rather than methane or other reduced species. A study on oxidation state of Hadean zircon suggests that such an environment was created as early as only within a few million years after core formation (Trail et al. 2011). Thus if magma ocean carbon ingassing requires the presence of a CO_2-rich atmosphere, then such a scenario was possibly created within few tens of million years after core formation.

But what if the carbon in the atmosphere existed as reduced gases such as methane? Zahnle et al. (2010) showed that an atmosphere generated by impact degassing would tend to have a composition reflective of the impacting bodies (rather than the mantle of the proto Earth), and these impactors tend to be strongly reducing and volatile-rich. A consequence is that, although CO- or methane-rich atmospheres are not necessarily stable as steady states, they quite likely have existed as long-lived transients, after a number of impacts. The other authors have also argued that Earth retained a significant portion of the impactors' atmosphere. For example, Genda and Abe (2003) studied a planet with a solid surface and found that after an impact
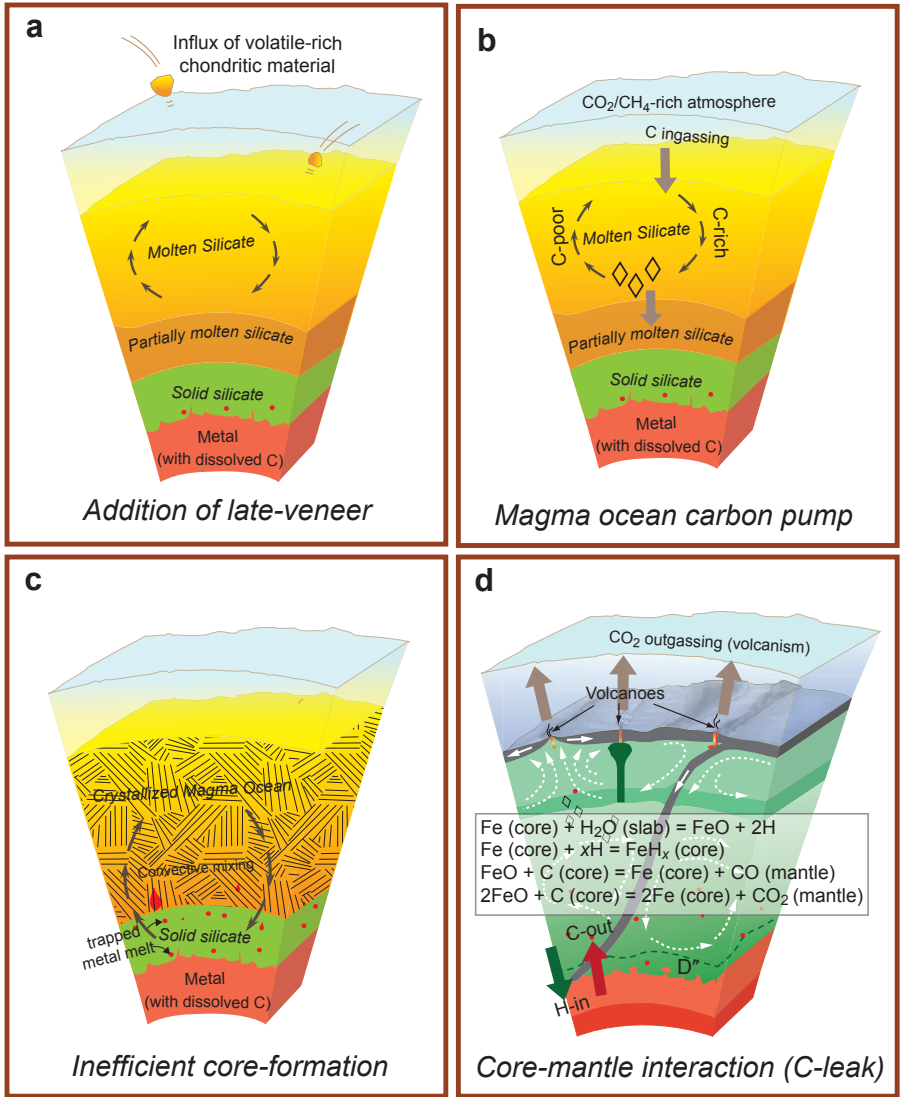
a

Influx of volatile-rich chondritic material

Molten Silicate

Partially molten silicate

Solid silicate

Metal
(with dissolved C)

Addition of late-veneer

b

CO_2/CH_4-rich atmosphere

C ingassing

C-poor   *Molten Silicate*   C-rich

Partially molten silicate

Solid silicate

Metal
(with dissolved C)

Magma ocean carbon pump

c

Crystallized Magma Ocean

Convective mixing

trapped *Solid silicate*
metal melt

Metal
(with dissolved C)

Inefficient core-formation

d

CO_2 outgassing (volcanism)

Volcanoes

Fe (core) + H_2O (slab) = FeO + 2H
Fe (core) + xH = FeH_x (core)
FeO + C (core) = Fe (core) + CO (mantle)
2FeO + C (core) = 2Fe (core) + CO_2 (mantle)

C-out

D"

H-in

Core-mantle interaction (C-leak)

Figure 5. Schematic cross sections illustrating the range of deep Earth processes from magma ocean stage of the Hadean Eon to the plate tectonic framework of the modern world, which may explain the "excess carbon" in the mantle. (a) Addition of volatile-rich materials to Earth after core formation has ceased. (b) Interaction between a magma ocean and carbon-rich proto-atmosphere to increase the C-budget of the magma ocean. (c) Convective mixing of C-rich lower mantle materials with the entire mantle, after the crystallization of the magma ocean. (d) Core-mantle interactions and possible back-release of C-bearing fluids/melts aided by the presence of "water"; introduction of water to core-mantle boundary regions may be aided by subduction.

of a Mars-sized body, Earth retained 70% of its atmosphere; if the impactor had only 10% Earth mass, Earth retained 80 to 90% of its atmosphere. Proto-Earth, therefore, could have had a more massive atmosphere following the impact than it had before and this atmosphere could have been more reduced. Planets with liquid surfaces are thought to lose far more of

their atmospheres during large impacts because of enhanced surface motion (Elkins-Tanton 2012). During the terrestrial magma ocean stage, large impacts thus would have removed large fractions of, but not the entire, atmosphere (Genda and Abe 2005). This atmosphere would then re-equilibrate with the magma ocean, causing magma to dissolve volatiles up to the solubility limits. Therefore, being struck by one or more reduced impactors, Earth could have inherited a methane-rich atmosphere, even if temporarily.

Could the magma ocean carbon ingassing operate with atmosphere being methane-rich rather than CO_2-rich? The depth dependence of methane solubility is ambiguous at present (Mysen et al. 2009; Ardia et al. 2011) but Dasgupta and co-workers (2012, 2013a) suggest that at graphite saturation, the total dissolved carbon that comprise more than one hydrogenated species of carbon (e.g., methane, methyl group, alkyne group) along with carbonates, also show a negative relationship with pressure. Hence, although somewhat speculative at this stage, magma ocean-atmosphere interaction may have acted as a carbon pump not only for a CO_2-rich atmosphere but also for a reduced (CH_4-bearing?) atmosphere.

Magma ocean crystallization and the fate of carbon. The above discussion suggests that although the core might have taken possession of most of Earth's carbon, a magma ocean-proto atmosphere interaction likely created an opportunity to restore the BSE carbon budget. Then the obvious next step to consider is the fate of the dissolved carbon in the magma ocean. The fate of dissolved carbon during crystallization of the terrestrial magma ocean depends on the Earth's temperature-f_{O_2} evolution. Because carbon solubility in reduced magma ocean drops precipitously with falling temperature (Fig. 4c), the storage capacity near the peridotite solidus can be 1-2 orders of magnitude lower than at temperatures relevant for magma oceans. Thus during crystallization of the magma ocean, diamond and graphite precipitation would take place as the peridotite solidus is approached. The temperature of precipitation of diamond/graphite in a cooling magma ocean would also depend on the depth of crystallization and the fugacity of hydrogen and water. Owing to decreased solubility of carbon as a function of increasing pressure, greater depths would see precipitation of diamond at a higher temperature. Thus if the crystallization of a well-mixed magma ocean proceeds within a narrow range of relatively reduced f_{O_2}, the lower part would tend to be more carbon-rich. Carbon enrichment in the lower part of the crystallizing magma ocean could be enhanced if magma ocean carbon ingassing also was efficient.

Carbon addition by late veneer? The late veneer, which has to be delivered after the latest stage of core formation, is widely considered to have added the refractory highly siderophile elements to silicate Earth (e.g., Chou 1978; Wänke and Dreibus 1988). A late veneer has also been invoked as a possible source for bulk Earth's or silicate Earth's water (Owen and Bar-Nun 1995; Morbidelli et al. 2000; Dauphas and Marty 2002; Albarede 2009; Marty 2012; Fig. 5a). It was also argued to be the main source of carbon and sulfur in silicate Earth (Yi et al. 2000). Addition of Earth's volatile elements by the late veneer has been suggested partly because of the premise that Earth may have lost most of its volatiles to space following a giant impact (Abe 1997; Genda and Abe 2003) and that the budget of terrestrial volatiles would therefore have to be reintroduced. But the proposition that BSE carbon is chiefly introduced by a "late veneer" is not entirely satisfactory.

In order to evaluate whether a "late veneer" could provide the bulk of Earth's carbon (and other volatiles), it is critical to evaluate how much of what types of materials were added and whether those additions satisfy the geochemistry of other siderophile elements. For example, the identical W isotopic composition of the Moon and the BSE has been argued to limit the amount of material that can be added as a late veneer to Earth after the giant impact to less than 0.3 ± 0.3 wt% of Earth's mass of ordinary chondrite or less than 0.5 ± 0.6 wt% CI-type carbonaceous chondrite based on their known W isotopic compositions (Halliday 2008). Similarly, the explanation of the mantle abundance of highly siderophile elements such as Pt and Pd seems

to limit the addition of chondritic veneer to ~0.7 wt% (Holzheid et al. 2000). Abundance levels as low as 0.003 × Earth mass and as high as 0.007 × Earth mass have been argued by other studies as well (Morgan et al. 2001; Drake and Righter 2002). Addition of 0.3-0.7% of CI-type chondrite with 3.5 wt% C (Lodders 2003) would add 105-245 ppm C (385-898 ppm CO_2; Fig. 6) to Earth after core formation had occurred. Although this range of carbon concentration may be sufficient to explain the carbon geochemistry of mantle domains as enriched as those of most plume source regions or the BSE estimate of McDonough and Sun (1995), it is distinctly less than the BSE carbon abundance of 765 ± 300 ppm as estimated by Marty (2012). Thus it may be difficult to invoke the addition of CI-type chondritic material to bring carbon levels of the post-veneer mantle to the levels needed to match BSE without increasing the highly siderophile elements rather more than they are seen to be in "excess."

Invoking CI-type carbonaceous chondrite as the agent of volatile and siderophile element delivery to the BSE is also problematic for the Os isotopic composition of the mantle, which matches that expected from a veneer with a Re/Os ratio like that of ordinary chondrites (Walker et al. 2002). Moreover, the Ru and Mo isotopic compositions of meteorites are correlated (Dauphas et al. 2004), and the BSE appears to be different from the composition of CI chondrites and more similar to ordinary chondrites (Drake 2005). One can go through a similar exercise to evaluate whether the ordinary chondrites can deliver the right concoction of
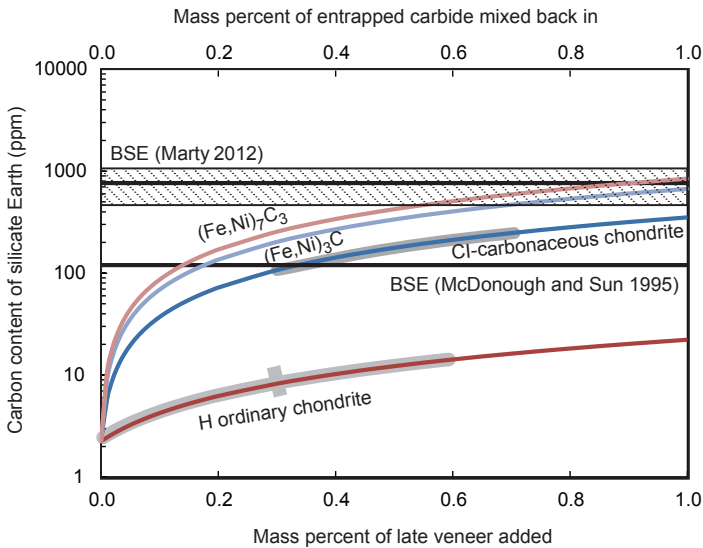

Figure 6. The effect of addition of chondritic late veneer and back-mixing of Fe-rich carbide from ineffi-cient core formation on the bulk mantle carbon budget. The suggested range of CI-carbonaceous chondrite addition as required by the refractory siderophile element budget of the mantle and W-isotopic composi-tion of the Earth-Moon system is highlighted in grey. The mean and standard deviation of the suggested value of ordinary chondrite addition are also highlighted in grey. Shown for reference are the BSE carbon estimate given by McDonough and Sun (1995) and Marty (2012). Plausible BSE carbon abundance of as much as 900-3700 ppm, i.e., even higher than the estimate of Marty (2012), exists in literature (Trull et al. 1993; Wood 1995; Wood et al. 1996) but are not plotted here for simplicity. The figure shows that if BSE carbon content of Marty (2012) or any other higher value is appropriate then the addition of chondritic "late veneer" cannot be the sole mechanism of bringing carbon to Earth. If on the other hand C-bearing core melt trapped in the lower mantle undergoes fractional crystallization, then some mantle domains could be Fe-carbide-bearing. Plotted, for example, are enrichments predicted for mixing such mantle domains con-taining stoichiometric $(Fe,Ni)_3C$ or $(Fe,Ni)_7C_3$ carbides. Admixing ~0.6 to 1.0 wt% of Fe-rich carbide can potentially elevate the magma ocean residual to core formation to the carbon level similar to that of BSE.

refractory siderophile elements and volatiles, including carbon. Halliday (2008) argued that in order to satisfy the W-isotopic composition of the BSE, no more than 0.3 ± 0.3 wt% of Earth's mass of H ordinary chondrite can be added. Thus with ordinary chondrite C content of 0.2 wt% (Moore and Lewis 1967), only ~6 ppm of carbon can be added through late veneer and hence cannot be a chief delivery agent to the BSE carbon budget.

Finally, if the BSE volatiles derive chiefly from a chondritic late veneer, it is also difficult to explain why the present-day H/C ratio of BSE (Hirschmann and Dasgupta 2009) is distinctly higher than all known chondritic materials (Kerridge 1985). Furthermore, carbon isotopic compositions of CI chondritic materials ($\delta^{13}C$~ −15 to −7‰) are distinctly lighter than the average carbon isotope composition of Earth's mantle ($\delta^{13}C$~ −5‰) (Kerridge 1985; Deines 2002). Therefore, any late delivery mechanisms may need to resort to more than one source that may be geochemically different than the known meteorites (Raymond et al. 2004; Raymond et al. 2006; Raymond et al. 2007; Albarede 2009); for example, carbonaceous chondrite and comets both may contribute differentially to the budget of carbon and water on Earth. In summary, although some parts of BSE carbon's delivery through a late veneer cannot be ruled out, it appears unlikely that late influx of chondritic materials is the primary process to elevate the carbon budget of the mantle after core formation.
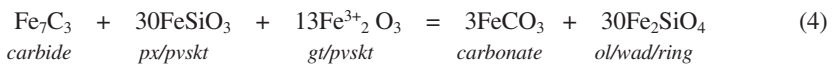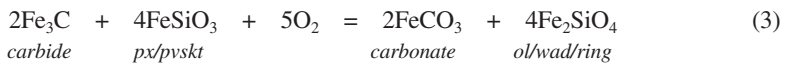
Inefficient core formation and deep carbon storage. Inefficient core formation has been invoked as a plausible mechanism for explaining the "excess" siderophile element abundance in the mantle by a number of authors (e.g., Jones and Drake 1986; Newsom and Sims 1991). Dasgupta et al. (2013a) suggested that a similar mechanism can be surmised to explain the "excess" carbon in the mantle. In this model, metallic liquid would drain inefficiently to join the core, so some small fraction of melt would be trapped in the solid mantle matrix, providing a source of carbon in the mantle (Figs. 1 and 5c). Interfacial energies between carbon-bearing metallic alloy melts and mantle minerals are not constrained at present but observed dihedral angles between many other metallic melt compositions and solid silicate minerals of >60° and mostly >90°-100° support such hypothesis (Minarik et al. 1996; Shannon and Agee 1996; Terasaki et al. 2007; Mann et al. 2008; Terasaki et al. 2008). Trapped Fe-rich, carbon-bearing metallic melt will provide a source for both refractory siderophile elements and carbon in the mantle. According to this suggestion of Dasgupta et al. (2013a), Earth's lower mantle could start off being more carbon-rich and solid state convection after magma ocean solidification would bring up the lower mantle material with accessory Fe-rich alloy, Fe-rich carbide, or C-bearing metallic alloy liquid (Fig. 5c). Dasgupta et al. (2013a) suggested that the exact chemical form of carbon storage in the solid lower mantle will depend on the phase relations of Fe-(±Ni)-C bearing metallic systems and the mantle adiabat of interest. Using the study of Lord et al. (2009) on Fe-C binary, Dasgupta et al. (2013a) noted that the key observations are: (1) with increasing pressure from 10 to 50 GPa, the solubility of carbon in crystalline-Fe likely diminishes and thus the probability of iron carbide stability increases; and (2) depending on the base of the magma ocean, the trapped core melt in the solid matrix at relatively shallower depths may exist as a molten alloy whereas at greater depths it will exist as either iron metal + cohenite ($Fe + Fe_3C$) or iron + Eckstrom-Adcock carbide ($Fe + Fe_7C_3$) assemblages.

The contribution of carbon dissolved in alloy or as Fe-rich carbide to the total budget of upper mantle carbon depends critically on its composition. If the trapped metallic melt undergoes batch freezing and has only modest carbon content, as will be the case if it is derived from equilibrium partitioning in a low bulk carbon environment, then its input to the present-day, upper mantle carbon inventory will be small. For example, if trapped metal with ~0.2 wt% C is only 0.1-1% of the lower mantle, then such a mantle domain will have only 2-20 ppm C (~7-73 ppm CO_2). It is not implausible, however, as argued above that in some mantle domains, that the trapped metallic liquid precipitates as Fe-rich carbide (e.g., Fe_7C_3 or Fe_3C solid solutions). Carbide formation is facilitated by the Fe-C eutectic composition becoming
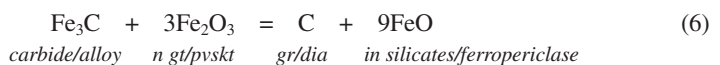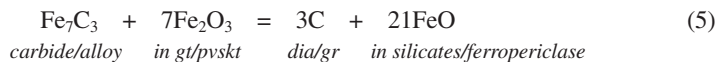
increasingly carbon-poor with increasing pressure (Wood 1993; Lord et al. 2009) and carbide-saturated Fe-alloy becoming poorer in carbon with increasing pressure (Walker et al. accepted). If separation of carbide from the remaining metallic liquid takes place, perhaps aided by the presence of silicate partial melts, then some lower mantle domains can be quite carbon-rich. If the lower mantle domain contains 0.1-1 wt% of Fe_7C_3, then such parcels can deliver ~84-840 ppm C (~310-3100 ppm CO_2) and convective mixing of only 10% of such mantle mass can contribute >30-300 ppm CO_2 to the Earth's depleted upper mantle (Fig. 6). It can be seen from Figure 6 that trapped carbide fractions have greater leverage, compared to delivery of late chondritic veneer, in supplying carbon to a depleted mantle. Another way to have the trapped core liquid be rich in carbon is to have carbon partitioning with a relatively low alloy:magma ocean mass ratio. For example, if only 20% of the core mass equilibrated with the whole mantle mass magma ocean, then the equilibrated alloy liquid could have had carbon content as high as 1 wt% (Fig. 3) even with a bulk Earth carbon as low as 730 ppm. Therefore, if volatile delivery was delayed to the latter part of accretion and if low alloy:magma ocean ratio was the norm for carbon fractionation, trapped core liquid can be quite C-rich.

If core-forming alloy liquid indeed provided some initial carbon, then the carrier phase of interest can be much more complex than that captured by the Fe-Ni-C system alone. For example, what if the segregating liquid alloy is also sulfur bearing? In such a case, phase relations of Fe-Ni-C-S systems will have to be considered. In that case diamond saturation may be achieved, owing to lower solubility of carbon in sulfide-rich melt (see the later discussion on carbon storage in the present-day mantle). Similarly, if the alloy liquid of interest is Si-bearing, phase relations in the Fe-Ni-Si-C system may come into play. In the latter case, crystallization of moissanite (SiC) in a reduced lower mantle cannot be ruled out. Although rarely found, moissanites have been reported as inclusions in natural diamonds (Leung et al. 1990; Leung 1990). If segregating alloy liquid crystallizes diamond and/or moissanite in the lower mantle, mixing of such mantle materials will be far more effective in bringing the bulk mantle carbon budget up.
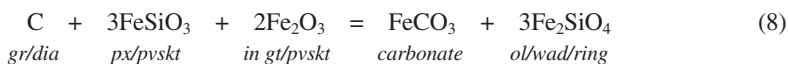
Transfer of carbon in trapped reduced phases by convective and oxidative processes. If core-forming liquid trapped in the lower mantle mineral matrix is the chief source of carbon in Earth's mantle in general, and in present-day Earth's upper mantle in particular, then some form of oxidative process is necessary for carbon to be mobilized from these reduced accessory phases. The following end-member reactions can be posited for such oxidative release of carbon:

$$2Fe_3C \ + \ 4FeSiO_3 \ + \ 5O_2 \ = \ 2FeCO_3 \ + \ 4Fe_2SiO_4 \qquad (3)$$
$$\textit{carbide} \quad \textit{px/pvskt} \qquad\qquad\quad \textit{carbonate} \quad \textit{ol/wad/ring}$$

$$Fe_7C_3 \ + \ 30FeSiO_3 \ + \ 13Fe^{3+}_2O_3 \ = \ 3FeCO_3 \ + \ 30Fe_2SiO_4 \qquad (4)$$
$$\textit{carbide} \quad \textit{px/pvskt} \quad\ \textit{gt/pvskt} \qquad \textit{carbonate} \quad \textit{ol/wad/ring}$$

where carbide reflects either a true Fe-rich carbide phase or a C-bearing component in the Fe-rich metal alloy and $Fe^{3+}_2O_3$ reflects a component in garnet (*gt*) or perovskite (*pvskt*), recognizing the highest Fe^{3+} uptake by these silicate phases (Frost et al. 2004; Rohrbach et al. 2011). Fe_2SiO_4 also reflects an end-member component in olivine (*ol*), wadsleyite (*wad*), or ringwoodite (*ring*) whereas $FeCO_3$ reflects either a component in a crystalline carbonate or a component in a carbonitic or carbonated silicate melt. Furthermore, oxidation of metal alloy or metal carbide likely does not directly generate carbonate or CO_2; more likely it proceeds through an intermediate stage of metal oxidation and diamond/graphite (*dia/gr*) precipitation (Frost and McCammon 2008) such as:

$$Fe_7C_3 \ + \ 7Fe_2O_3 \ = \ 3C \ + \ 21FeO \qquad (5)$$
$$\textit{carbide/alloy} \quad \textit{in gt/pvskt} \quad \textit{dia/gr} \quad \textit{in silicates/ferropericlase}$$

$$Fe_3C \ + \ 3Fe_2O_3 \ = \ C \ + \ 9FeO \qquad (6)$$
$$\textit{carbide/alloy} \quad \textit{n gt/pvskt} \quad \textit{gr/dia} \quad \textit{in silicates/ferropericlase}$$

followed by oxidation of graphite/diamond through reactions of the sort:

$$C + Fe_2SiO_4 + O_2 = FeCO_3 + FeSiO_3 \qquad (7)$$
$$\text{gr/dia} \quad \text{ol/wad/ring} \qquad\qquad \text{carbonate} \quad \text{px/pvskt}$$

$$C + 3FeSiO_3 + 2Fe_2O_3 = FeCO_3 + 3Fe_2SiO_4 \qquad (8)$$
$$\text{gr/dia} \quad \text{px/pvskt} \quad \text{in gt/pvskt} \quad \text{carbonate} \quad \text{ol/wad/ring}$$

Again, all of the above reactions are shown with both oxygen and Fe^{3+} as oxidants. Rohrbach and Schmidt (2011) showed that the transition from a metal and diamond-bearing mantle to a carbonated mantle takes place at ~250 km depth for a geotherm relevant to the present-day sub-ridge environment. If this depth was relevant for the mantle soon after magma ocean crystallization, then oxidative release of carbon from metal alloy and/ or carbide would have taken place somewhat above the mantle transition zone. However, the proportion of metal alloy/ carbide that might be physically entrapped in solid silicate matrix of the lower mantle can be more than the metal proportion of ~1 wt% expected by Fe^{2+} disproportionation in the present-day lower mantle (Frost et al. 2004) and much more than 0.1 wt% supposedly present in the modern deep upper mantle. Similarly, the composition of the trapped metal and/or metal carbide phase may have much higher Fe/Ni ratio compared to those formed by iron disproportionation. Hence the buffering capacity of such metal alloy/carbide-rich mantle may be different than what is predicted for present-day Earth's metal-poor mantle below ~250 km (Rohrbach et al. 2007, 2011). Future experiments will need to constrain the conditions of redox reactions involving variable metal alloy compositions.

CARBON RETENTION: MODULATING MANTLE CARBON BUDGET THROUGH THE WILSON CYCLE

The preceding discussion sheds some light on the path for attaining the inventory of mantle carbon in general and that of the upper mantle in particular. It was argued that it is possible to conceive a set of processes that yield carbon content similar to that of the present-day budget by late Hadean to early Archean time. If Earth's mantle attained a carbon content similar to the BSE inventory early in its life, how is such a budget maintained and processed in the light of the ongoing differentiation of the planet for more than 4 Ga? While magma ocean processes dominated the proceedings of deep carbon cycle in the Hadean, the carbon cycle post magma ocean crystallization was modulated by the thermal vigor of solid state convection and plate tectonic cycles. In this section, the current thinking of Earth's deep carbon cycle in the plate tectonic framework of mantle differentiation is reviewed. It will be shown that the mantle inventory of carbon may have gone through definite changes as a function of time, between the Archean Eon and the present-day and that key processes that affected such changes are the efficiency of crustal carbon recycling and the efficiency of CO_2 release through partial melting in oceanic provinces, both of which are controlled by the evolving thermal state of Earth's mantle at various tectonic settings. For magmatic outgassing of carbon, the key parameter of interest is the depth of onset of decompression melting and the extent of melting; the deeper and higher the extent of partial melting of the mantle, greater is the efficiency of carbon liberation (e.g., Dasgupta and Hirschmann, 2006; Dasgupta et al. 2013b). For recycling of crustal carbon, the key factor is the relative positions of decarbonation and decarbonation melting reactions of the lithospheric lithologies and depth-temperature paths of downgoing lithospheric materials. If at shallow depths (e.g., sub-arc depths), the former are cooler compared to the latter then one would predict inefficient deep subduction of carbon with most carbon being stripped off from the downgoing slab and released back to the exosphere by arc magmatism. If, on the other hand, up to the sub-arc depths the downgoing lithologies experience temperatures cooler than the key decarbonation reactions, then carbon hosted in lithosphere is expected to avoid the magmatic release in the volcanic arcs and participate in the deeper cycling and mantle processes.

Carbon cycle in an ancient Earth with greater thermal vigor: an era of more efficient outgassing?

A number of naturally relevant composition studies based on ancient rock records suggest that Earth's mantle was hotter in the Archean through Proterozoic time (Herzberg et al. 2010; Lee et al. 2010). While the average mantle potential temperatures (T_P) relevant for modern Earth is estimated to be ~1300-1400 °C (e.g., Ita and Stixrude 1992; McKenzie et al. 2005; Herzberg et al. 2007; Herzberg and Asimow 2008), basalt genesis from non-arc settings at 2.5-3.0 Ga requires that the potential temperatures were at least 1500-1600 °C. If Archean komatiites are considered, then the relevant mantle potential temperatures would be at least 1700 °C (Herzberg et al. 2010; Lee et al. 2010). The question then is how deep was the onset of decompression melting in the Archean-Proterozoic time. Decompression melting beneath mid-oceanic ridges, which particularly controls the release of carbon and other highly incompatible elements, is the depth of carbonated peridotite solidus. Figure 7 shows a compilation of experimental data that
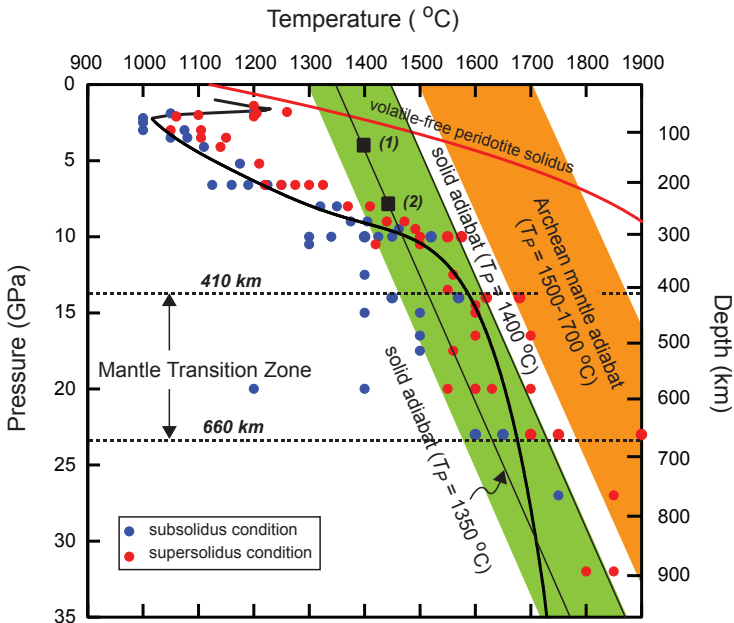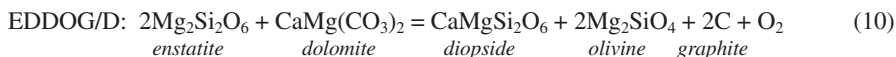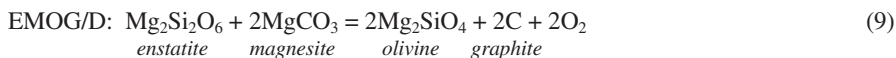

Figure 7. Experimentally constrained solidus of nominally anhydrous, carbonated fertile peridotite. The experiments include those from Falloon and Green (1989) at 1.4-3.5 GPa, Dasgupta and Hirschmann (2006) at 3.0-10.0 GPa, Dasgupta and Hirschmann (2007a) at 6.6 GPa, Ghosh et al. (2009) at 10.0-20.0 GPa, Litasov and Ohtani (2009) at 16.5-32.0 GPa, and Rohrbach and Schmidt (2011) at 10-23 GPa. The shape of the solidus over 3-10 GPa pressure range is constrained by the experiments of Dasgupta and Hirschmann (2006), but the exact location is adjusted to that expected for a peridotite with ppm level CO_2 after Dasgupta and Hirschmann (2007a). Subsolidus and supersolidus experiments are given by solid blue and open red circles, respectively. The preferred solidus from 2 to 35 GPa is fitted with a polynomial. Unlike in the study of Dasgupta and Hirschmann (2010), where the solidus at >10 GPa was parameterized by correcting for the bulk compositional differences between the studies performed at lower (≤10 GPa; natural fertile peridotite compositions) and higher (≥10 GPa; fertile peridotite with excess alkalis or peridotite in the simple system CMASN+CO_2) pressures, here the solidus at >10 GPa is parameterized by using the brackets from the study of Rohrbach and Schmidt (2011). Also shown for reference (black boxes on the 1350 °C mantle adiabat) are the conditions of redox melting as proposed by (1) Stagno and Frost (2010) and (2) Rohrbach and Schmidt (2011). The green and saffron shaded bands indicate approximate location of the solid mantle adiabats of the modern mantle (T_P = 1300-1450 °C) and the Archean mantle (T_P = 1500-1700 °C), respectively.

constrains the solidus of carbonated fertile peridotite solidus. At depths in excess of ~70 km, the carbonated peridotite solidus is 350-500 °C cooler than that of volatile-free solidus. The shape of the solidus is such that it intersects the solid mantle adiabat for T_P of 1350 °C at ~10 GPa. Thus, in modern Earth's upwelling carbonated mantle, melting initiates at a minimum depth of ~300 km. Another curious feature of the fertile carbonated peridotite solidus is that it changes slope sharply at ~10 GPa and remains similar to the solid mantle adiabat with T_P of ~1350-1400 °C at higher pressures. Hence adopting any hotter mantle adiabat for the Archean and part of the Proterozoic (Herzberg et al. 2010) would predict that the entire mantle may have possibly remained above the carbonated peridotite solidus. The implication is that the mantle can be very efficiently processed through the carbonated peridotite solidus.

But is the hotter thermal state of the mantle the only factor affecting the depth of onset of partial melting and carbon release? In order to use the depth of intersection of solid mantle adiabats and carbonated peridotite solidus as the depth of first melting in the adiabatically upwelling mantle, carbon in peridotite is required to be stored as mineral carbonates (e.g., Falloon and Green 1989; Dalton and Presnall 1998; Dasgupta and Hirschmann 2006; Dasgupta and Hirschmann 2007a). However, carbon in the mantle can be stored not only as mineral carbonates (magnesite and dolomite solid solution for mantle peridotite) but also as graphite or diamond (Eggler and Baker 1982; Eggler 1983; Luth 1993; Luth 1999; Dasgupta and Hirschmann 2010; Rohrbach and Schmidt 2011; Dasgupta et al. 2013b). Therefore, the depth of onset of melting must vary as a function of the mode of carbon storage. Two factors critically affect whether carbon in the mantle at depths is being stored in carbonates or in one of the reduced phases: (1) the locations of the equilibrium reactions that constrain the stability of carbonate versus graphite/diamond in P-T-f_{O_2} space, and (2) the oxygen fugacity profile of the mantle as a function of depth.

(1) Equilibrium reactions. Carbonate-carbon (graphite:G or diamond:D) equilibria involving upper mantle silicates at subsolidus conditions have long been constrained (Eggler and Baker 1982; Eggler 1983; Luth 1993).

EMOG/D: $Mg_2Si_2O_6 + 2MgCO_3 = 2Mg_2SiO_4 + 2C + 2O_2$ (9)
        enstatite   *magnesite*   *olivine*   *graphite*

EDDOG/D: $2Mg_2Si_2O_6 + CaMg(CO_3)_2 = CaMgSi_2O_6 + 2Mg_2SiO_4 + 2C + O_2$ (10)
        enstatite   *dolomite*   *diopside*   *olivine*   *graphite*

Reaction (9) also can be rewritten to constrain the oxygen fugacity at which magnesite coexists with diamond, clinoenstatite ($MgSiO_3$), and wadsleyite/ ringwoodite (Mg_2SiO_4) at transition zone depths (Stagno et al. 2011).

(2) Depth versus oxygen fugacity. The depth versus effective oxygen fugacity profile depends on the chemical species that are responsible for controlling the oxygenation potential of mantle assemblages. Silicate equilibria involving the exchange of Fe^{3+} and Fe^{2+} between silicate minerals could be responsible for controlling the apparent f_{O_2} (Gudmundsson and Wood 1995; Rohrbach et al. 2007; Frost and McCammon 2008) and in this case the chemical form of carbon will rely on the intersection of the iron redox state imposed f_{O_2} and the carbonate-carbon (graphite/diamond) transformation reactions. However, mantle f_{O_2} may also be buffered by carbon-carbonate equilibria (Eggler 1983; Luth 1999), in which case the stability of carbon versus carbonate and f_{O_2} versus depth are not controlled by the energetics of Fe^{3+} incorporation into silicate minerals such as garnet or perovskite (Gudmundsson and Wood 1995; McCammon 2005; Frost and McCammon 2008) but by the EMOD-type equilibrium (Equation 9). Although many studies have favored the Fe^{3+}-Fe^{2+} equilibria as the independent variable affecting effective f_{O_2} at depth, whether carbon-carbonate equilibrium buffers the f_{O_2} instead remains an open question. In particular, if the Hadean and Archean mantle was carbon-rich (owing to inefficient core formation or through magma ocean-atmosphere interaction or by addition of

late-veneer as discussed previously), then the buffering capacity of Fe^{3+}-Fe^{2+} in silicates might have been overwhelmed by that involving carbon (Luth 1999). Not having continental crusts of sufficient volume, the exospheric storage of carbon may have been limited and the entire of budget of BSE carbon might have been in the mantle (Marty and Jambon 1987). In fact, if the BSE carbon content (765-3700 ppm) estimated by Marty (2012) or by earlier works (Trull et al. 1993) applied to the whole mantle of the Hadean or Archean Eons, then carbon-carbonate equilibria would indeed control the f_{O_2} of the deep mantle. If this was the case then the first melting of the upwelling mantle would take place very deep in the mantle at the carbonated peridotite solidus.

Inefficient subduction of carbon in the Archean and Proterozoic?

The timing of initiation and the nature of tectonics involving ancient subduction zones are actively debated. The mineral assemblages included in diamonds spanning the past 3.5 billion years suggest that the subduction may have initiated at ~3.0 Ga (Shirey and Richardson 2011). Much older subduction-type environments have even been suggested based on thermobarometric estimates of the inclusions in 4.02-4.19 Ga zircons (Hopkins et al. 2008; Hopkins et al. 2010). If some form of lithospheric recycling initiated in the late Hadean to early Archean, then what was the thermal vigor of such ancient recycling processes and how did it evolve through the Archean and Proterozoic Eons? This question is crucial because in order to predict the subduction potential of carbon, the thermal profile of the downgoing plate as a function of depth needs to be known. Geodynamic predictions suggest that subduction may have initiated with T_P being as much as 175-200 °C hotter than of the modern Earth (Sizova et al. 2010). However, the increase in mantle potential temperature should not be directly reflected in the slab surface temperature. Hotter mantle would generate thicker crust and faster plate velocity, both of which would offset the effect of hotter mantle wedge temperature and therefore the slab surface temperature-depth trajectories of ancient subduction may not be much hotter. These geodynamic considerations suggest that the temperature during subduction may have been ~87-100 °C (50% of the potential temperature) hotter (van Keken personal communication). In addition to the geodynamic predictions, the estimates of ancient geothermal gradient based on thermobarometry of Precambrian rock records also exist (e.g., Nakajima et al. 1990; Möller et al. 1995; Komiya et al. 2002; Brown 2006; Moyen et al. 2006; Mints et al. 2010; Saha et al. 2010). In Figure 8, following the approach of Dasgupta and Hirschmann (2010) and Tsuno and Dasgupta (2011), the plausible depth-temperature trajectories experienced by subducting rocks during the Archean-Proterozoic are compared with the experimental constraints on decarbonation reactions (CO_2-rich fluid or carbonated melt liberation) of subducting lithologies. Subduction zone thermal conditions based both on geodynamic and petrologic constraints are presented. It can be noticed that the estimates derived from the rock records suggest higher subduction zone temperatures than those predicted by geodynamic modeling. For simplicity only one plausible *P-T* trajectory of ancient subduction that is hotter than Cascadia subduction zone by 100 °C is plotted. This estimate is most likely at the upper end of all the ranges slab-surface temperatures, given that most other modern subduction zones are cooler than that of Cascadia. Therefore, the difference between the geodynamic predictions and natural rock records is likely even more than what appears in Figure 8.

The compositions and the relative proportions of carbon-bearing rock types during this ancient time-period are poorly constrained and in Figure 8 it is assumed that all the three dominant carbonated lithologies that subduct in modern Earth—that is carbonated ocean floor sediments, carbonated altered basalt, and carbonated peridotite (ophicarbonate)—participated in the subduction-type environment of deep time, although their relative importance in terms of the flux of carbon in the downgoing slab may have been different than what has been estimated for modern subduction zones globally (Sleep and Zahnle 2001; Jarrard 2003; Dasgupta and Hirschmann 2010).
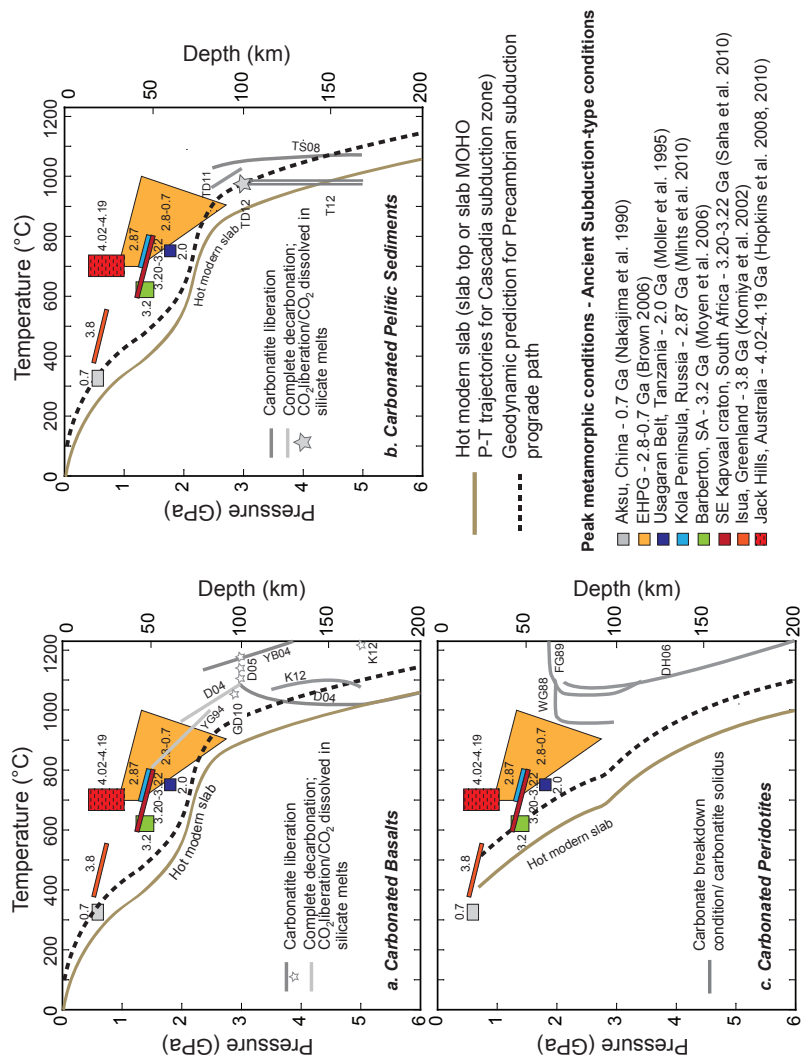
Figure 8. Comparison of subducting slab *P-T* estimates for the Hadean to Proterozoic subduction-type environment and experimentally constrained equilibria of decarbonation and carbonate melting of: (a) carbonated basaltic crust; (b) carbonate-bearing pelitic sediments; and (c) carbonated (lithospheric) mantle peridotite. *P-T* estimates relevant for ancient subduction zones come from thermobarometric estimates from various ancient rocks. Ages from various studies are marked next to the *P-T* estimates. The data from Hopkins et al. (2008; 2010) are tagged with a stippled area because, although these data call for a subduction-type environment in the Hadean Eon, it is unclear whether the *P-T* estimates reflect thermal conditions of downgoing slab. Also included for comparison are the estimates of slab-top depth-temperature trajectory (in a and b) and crust-mantle lithosphere interface depth-temperature trajectory (in c) of Cascadia subduction zone ("hot modern slab"; (Syracuse et al. 2010) and a plausible hot subduction of Archean age, which is 100 °C hotter and has a similar topology of the Cascadia *P-T* paths. Decarbonation melting conditions for basalt-hosted carbonates in (a) come from the studies of (Y94) Yaxley et al. (1994), (D04, D05) Dasgupta et al. (2004, 2005), (YB04) Yaxley and Brey (2004), (GD10) Gerbode and Dasgupta (2010), and (K12) Kiseeva et al. (2012). Carbonate-out boundaries for subducting pelites in (b) come from the studies of (TS08) Thomsen and Schmidt (2008), (TD11, TD12) Tsuno and Dasgupta (2011, 2012), and Tsuno et al. (2012) and for carbonated peridotite (±H$_2$O) in (c) from the studies of (WG88) Wallace and Green (1988), (FG89) Falloon and Green (1989), and (D06) Dasgupta and Hirschmann (2006). For clarity only the complete decarbonation and carbonatite melting boundaries are shown. The complete near-solidus relations involving silicate melting are not included.

Legend (figures a and b):
- Carbonatite liberation
- Complete decarbonation; CO$_2$ liberation/CO$_2$ dissolved in silicate melts

Legend (figure c):
- Carbonate breakdown condition/carbonatite solidus

a. Carbonated Basalts
b. Carbonated Pelitic Sediments
c. Carbonated Peridotites

- Hot modern slab (slab top or slab MOHO)
- P-T trajectories for Cascadia subduction zone
- Geodynamic prediction for Precambrian subduction prograde path

Peak metamorphic conditions - Ancient Subduction-type conditions
- Aksu, China - 0.7 Ga (Nakajima et al. 1990)
- EHPG - 2.8-0.7 Ga (Brown 2006)
- Usagaran Belt, Tanzania - 2.0 Ga (Moller et al. 1995)
- Kola Peninsula, Russia - 2.87 Ga (Mints et al. 2010)
- Barberton, SA - 3.2 Ga (Moyen et al. 2006)
- SE Kapvaal craton, South Africa - 3.20-3.22 Ga (Saha et al. 2010)
- Isua, Greenland - 3.8 Ga (Komiya et al. 2002)
- Jack Hills, Australia - 4.02-4.19 Ga (Hopkins et al. 2008, 2010)

Figure 8b shows that on average, at any given pressure, carbonated pelitic sediments have the lowest decarbonation and carbonate melting temperatures, thus they are most prone to losing their carbon inventory during subduction. Carbonated ocean floor basalts or their derivatives, carbonated eclogite, have intermediate decarbonation or carbonate melting temperatures and carbonated peridotites have the highest carbonate melting solidi. Thus if a slab surface *P-T* trajectory hotter by ~100 °C than the hottest subduction zone of modern Earth (Cascadia) is considered, then compositions similar to carbonated silicate sediments of the present-day ocean floor will be completely carbon-free by carbonate melting or decarbonation by depths of ~100-150 km. Whereas if metamorphic conditions recorded in ancient crustal assemblages rightly capture the prograde subduction path of the Precambrian, then sediment decarbonation may have been completed as shallow as 80-100 km. These depth estimates are well within modern Earth sub-arc depths of 72-179 km (Syracuse and Abers 2006).

With *P-T* conditions similar to those recorded in the Precambrian rock record, altered ocean floor basalts would undergo complete decarbonation by 80-120 km (Yaxley and Green 1994; Dasgupta et al. 2004; Yaxley and Brey 2004; Dasgupta et al. 2005; Gerbode and Dasgupta 2010; Kiseeva et al. 2012). Whereas if slab-top temperatures were only up to 100 °C hotter than the hottest subduction zone of the present era, then carbonated basaltic compositions, which stabilize calcitic crystalline carbonate in the eclogite (Yaxley and Green 1994; Yaxley and Brey 2004; Dasgupta et al. 2005), would survive significant decarbonation in the Precambrian sub-arc depths (Fig. 8a). Under similar conditions, basaltic eclogites with more magnesian crystalline carbonate (dolomite to magnesite solid solution), would undergo complete decarbonation and carbonate melting by 125-170 km depth (Dasgupta et al. 2004; Dasgupta et al. 2005; Gerbode and Dasgupta 2010).

The fate of carbon hosted in oceanic mantle lithosphere is somewhat unclear, partly because of the fact that compositions that derive from serpentinized and carbonated depleted peridotite have not been extensively studied experimentally. Also, compositions representative of serpentinized carbonated peridotite and their dehydrated products (fluid-absent, carbonated peridotite) are poorly constrained. In terms of the phase relations of altered lithosphereic mantle, what exist are thermodynamic calculations relevant for low-pressure devolatilization of ophicarbonates (Kerrick and Connolly 1998) and melting and decarbonation relations of more fertile peridotite compositions under hydrous (Wallace and Green 1988) or nominally anhydrous (Falloon and Green 1989; Dasgupta and Hirschmann 2006; Dasgupta and Hirschmann 2007a) conditions. If these phase relations are a reasonable approximation of high-pressure behavior of carbonated lithosphere, then subducting mantle likely had the best prospect of carrying carbon down deep. This conclusion follows because peridotitic lithologies provide the greatest thermal stability of crystalline carbonates and they go down along the coolest paths during subduction (Fig. 8c).

Although Precambrian subduction can be argued to be hotter on average than modern Earth, what remains uncertain is the time scale over which slab thermal structure evolved to something similar to that of the present day. Figure 9a presents a conjectural projection of all the various temperature estimates for subduction-type environments between the Archean Eon and Neoproterozoic Era to a constant depth of ~70 km. The different *P-T* estimates are projected to a single pressure of ~2 GPa, using the topology of the slab surface *P-T* path estimated for the present-day subduction zone in Cascadia. Although for comparison with experimental data of decarbonation/melting, slab temperatures at somewhat higher pressures are necessary, *P* = 2 GPa is preferred to avoid significant extrapolation of the available thermobarometric data, which record peak metamorphic temperatures at *P* ≤ 2.5 GPa and mostly < 2 GPa. However, Figure 9a does shed some light on the extent of excess temperature that the downgoing crustal rocks of Precambrian likely have suffered compared to those that subduct in modern Earth. It shows that slab temperatures were likely hotter by as much as 100 °C as recently as 1 Ga even
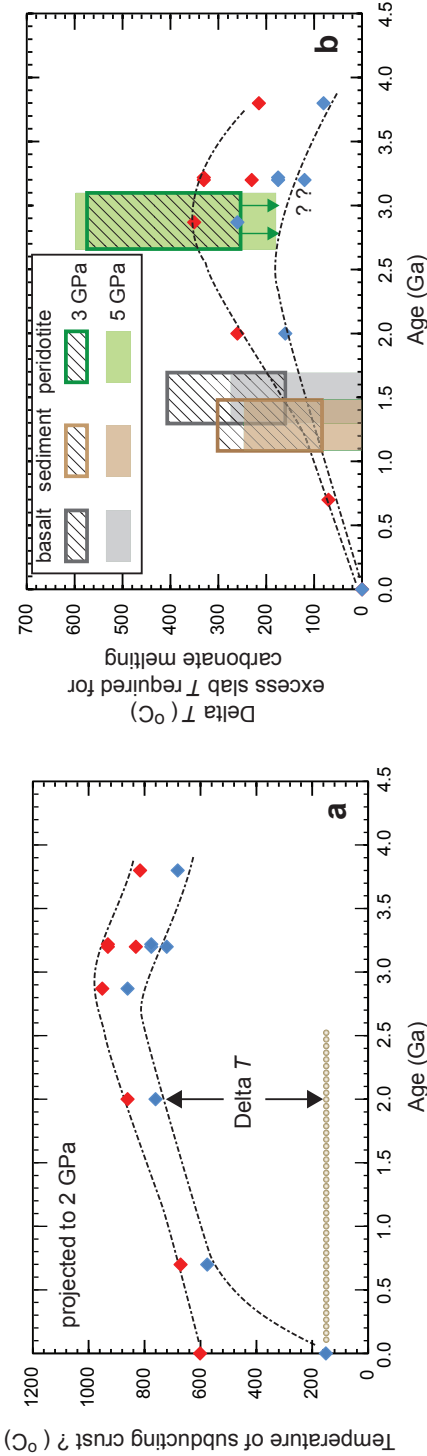
Figure 9. Subduction potential of carbonated lithologies from the Archean Eon to the present by comparing subducting slab *T* estimates through time and experimentally constrained *T* of decarbonation and carbonate melting. (a) The range of metamorphic temperatures as a function of age for various subduction zone crustal assemblages. The temperature estimates are based on thermometry and are taken from the literature data given in Figure 8 legend and in the text. The actual *P-T* estimates from Figure 8 are projected to a constant pressure of 2 GPa for the ease of comparison. The red and the blue diamonds represent the maximum and minimum temperatures, respectively, projected from each study plotted in Figure 8. The present-day (0 Ga) subducting slab temperature range reflects the slab-surface temperatures for Cascadia (max *T*) and the average of all the intermediate to cold subduction zones (min *T*). Although highly speculative, these data suggest that the subduction zones globally may have cooled substantially throughout Earth's history. The "Delta *T*" indicates the excess slab temperature applicable for subduction of a given age. (b) Excess slab temperature required to cause decarbonation/melting of a given lithology at 3 and 5 GPa versus the excess slab temperature of ancient to modern subduction zones as constrained in (a). The former is estimated by the difference between the range of experimental temperatures of carbonate out boundaries and the expected temperature of the lithology during subduction. For sediments and basaltic crust the temperature during subduction is taken as the slab-top temperature for a depth of interest (i.e., the maximum *T* experienced by these lithologies) and for mantle lithosphere the temperature at the base of 7 km thick oceanic crust is used. For the behavior of carbonated sediments, slab-surface temperatures between the average of all subduction zones where carbonated sediments subduct globally (Sunda, Vanuatu, Nicaragua, Lesser Antilles) and the hottest slab surface temperature known (Cascadia) are used. For consistency, the same range of slab surface temperatures are used for constraining the behavior of carbonated ocean crust. To constrain the fate of carbonate-bearing mantle lithosphere (ophicarbonates), the temperatures at the base of the oceanic crust are used from the same subduction zones (i.e., Sunda, Vanuatu, Nicaragua, Lesser Antilles, and Cascadia). The position of each of these lithologies on the *x*-axis reflects the age where approximately half of the 5 GPa "Delta *T*" estimates for the given lithology falls below the trend of "Delta T" indicated by ancient subduction zones. Based on this comparison, it appears that subduction zones may have cooled enough by ~1.5 Ga and ~1.3 Ga to not force decarbonation or carbonated melting of basaltic crusts and sediments, respectively at sub arc depths, whereas if the top of mantle lithosphere was carbonated then such lithology would remain unsusceptible to decarbonation even in the early Archean Eon.

if the hottest subduction zone of modern Earth is used as a reference (Fig. 9). If the trend of excess slab temperature versus age is followed, then it appears that many carbonated sediment and carbonated ocean floor basalt compositions likely suffered sub-arc depth decarbonation and carbonated partial melting in all of the late Hadean Eon, the Archean Eon, and perhaps at least the first half of the Proterozoic Eon. Only as recently as 1.2-1.5 Ga does subduction appear to be cold enough to allow significant subduction of crustal carbonate beyond sub-arc depths of 100-170 km. However, depending on the choice of carbonated crust compositions, some deep subduction likely took place even earlier. Ophicarbonates could, however, have subducted even during the Archean-Proterozoic time as the *P-T* trajectories of mantle lithosphere, which are cooler than the overlying crust, likely remained significantly below the solidi temperatures of carbonated ($\pm H_2O$) peridotite (Fig. 9b). If the most recent estimate of serpentinites-hosted carbon content (500-1000 ppm C; primarily in the form of sea-water carbonates and smaller fractions of organic carbon; (Alt et al. 2012) is considered as a relevant estimate for the ancient subduction, then with serpentinites making up 10% of the 10-km thick layer of suboceanic mantle, an estimated 4.8-9.6×10^{12} g C/yr would be added to the subducting assemblage. Considering the present-day input of carbon through subduction of altered oceanic crust alone is ~6.1×10^{13} g C/yr, the contribution of carbon hosted in the mantle section of the Archean Eon would have been about an order of magnitude lower. Future studies will have to constrain the abundance of mantle-hosted carbon in the Archean and Proterozoic lithospheric sections in order evaluate the potential role of mantle subduction in deep carbon cycle of the Archean Eon.

Another possibility of somewhat enhanced subduction of carbonate in the Precambrian is that, owing to higher solidi of carbonated peridotite with respect to carbonated basalt and sediments, some fraction of released CO_2/carbonate melt may freeze in the mantle wedge peridotite immediately above the downgoing slab. If this was the case, this hanging wall peridotite can be dragged down into the deeper mantle along with the subducting slab. It is unclear how much carbon may get locked into peridotite in this fashion, because crystalline carbonate stability in compositions relevant for carbonated slab melt influxed peridotite is unconstrained. Likewise, despite the thermal hindrance to early Earth carbonate subduction, subduction of reduced carbon may have been another mechanism for carbon ingassing in the Hadean, as graphite/diamond has no notable effect on the solidus of dry mantle lithologies. This idea gains support from the fact that a significant fraction of near-surface carbon could have been graphite or other reduced phases in early Earth (Catling et al. 2001).

The above discussion suggests that, owing to somewhat more efficient decarbonation of the subducting crusts at relatively shallow depths, the flux of CO_2 through Archean volcanic arcs likely was higher and deep subduction of carbon may have been hindered. In addition, owing to Earth's much hotter conditions, the subduction cycles may have also been episodic in nature for most part of the Precambrian (O'Neill et al. 2007; Moyen and van Hunen 2012), thus making subduction introduction of crustal carbon to the mantle even a less reliable ingassing process.

Petrologic solution to Faint Young Sun Paradox — the role of arc volcanism. A corollary of the discussion in the preceding section is that during the Hadean to Mesoproterozoic time the majority of Earth's carbon that did not segregate to the core, or was lost to space during accretion, was likely restricted to the exosphere (crust + atmosphere) with only a limited cycling involving the shallow mantle wedge. The convecting mantle's carbon-poor state would be exacerbated by the fact that carbon outgassing may have been more efficient with deeper carbonated melting. This prediction of more efficient subduction decarbonation (along with deep carbonated melting beneath oceanic volcanic centers) or at least less systematic subduction must have had important implications for the Faint Young Sun Paradox (Sagan and Mullen 1972; Feulner 2012). This paradox describes the apparent contradiction between geologic evidence of liquid water on Earth's surface as early as Hadean time and the astrophysical expectation that the Hadean Sun was ~30% less luminous than today at ~4.6 Ga (Sagan and

Mullen 1972) and remained at least 10% less luminous as recently as 1.5 Ga (Gough 1981). If atmospheric chemistry was the same as that of modern Earth, with Sun's output being only 70-90% of that of the modern epoch, Earth's surface temperature (T_s) would remain <273 K (Budyko 1969; Kasting and Catling 2003; Zahnle 2006; Zahnle et al. 2007), thus preventing water to exist in the liquid form as recently as 1.5-2.0 Ga (Kasting and Catling 2003). One of the ways to get around this problem is to have higher concentrations of atmospheric CO_2 than modern Earth's (preindustrial) nominal value of ~300 ppmv (Owen et al. 1979; Walker et al. 1981; Kuhn and Kasting 1983). However, although higher partial pressure of CO_2 in the ancient terrestrial atmosphere is a popular model, little has been discussed in literature about the source of excess volcanic CO_2 (Feulner 2012).

The comparison between the estimated temperatures of Precambrian subduction zones and the high-pressure experimental phase relations of crustal decarbonation suggests that significant CO_2 liberation at volcanic arcs likely helped to sustain higher CO_2 content in the exosphere for at least 2.5 billion years, between ~4 Ga and 1.5 Ga (Fig. 9b). Although the role of volcanic CO_2 as the main greenhouse gas required to offset the lower solar luminosity has been speculated before, the analyses presented here suggests that it specifically was CO_2 outgassing at ancient arcs that likely provided the excess CO_2. But how much carbon was released to atmosphere through arc volcanism during the Archean Eon? Similar to the present-day, carbonated basaltic crust likely was the chief source of crustal carbon entering ancient subduction zones. In present-day Earth, carbonate precipitated as veins and present in vesicles in the upper volcanics of ocean floor basalt amounts to ~0.3 wt% CO_2 of the 7 km thick ocean crust (Alt and Teagle 1999; Alt 2004). For a subduction rate of 3 km^2/yr, relevant for the Phanerozoic Eon (Reymer and Schubert 1984), this equates to subduction of 6.1×10^{13} g of C/yr (2.2×10^{14} g of CO_2/yr) (Dasgupta and Hirschmann 2010): all of which could have potentially been released in the Archean Eon. With greater vigor of hydrothermal activity and faster sea-floor spreading, the carbonation rate of the Archean ocean crust and flux of carbon to subduction zones could have been more extreme, however. For example, the study of Nakamura and Kato (2004) on the top 500 m of early Archean (3.46 Ga) hydrothermally altered basaltic rocks exposed near the Marble Bar area of the eastern Pilbara Craton, Western Australia, suggests that the carbon flux to subduction zones at this time period was ~4.6×10^{14} g of C/yr (~1.7×10^{15} g of CO_2/yr). Shibuya and co-workers (2012) investigated the Cleaverville area of Pilbara Craton and constrained carbonation of the top 4000 m of the middle Archean MORB-like greenstone composition. This latest study yielded an even more extreme flux of subducting carbon of ~1.8×10^{15} g of C/yr (6.6×10^{15} g of CO_2/yr). Again, all of this carbon being outgassed at volcanic arcs would yield at least 1-2 orders of magnitude higher flux than the total flux of modern volcanic CO_2 emission, with all magmatic centers combined.

Punctuation of the deep carbon cycle of the Precambrian by supercontinent formation?
The preceding section suggests that breakdown and outgassing of recycled crustal carbonates at volcanic arcs were perhaps much more frequent in most of the Precambrian and this process may have implications for the Faint Young Sun paradox. If this was the case, does it mean there was very limited deep ingassing of crustal carbonates through the Precambrian? Were the subduction zones hot throughout the Archean and early Proterozoic Eons? The thermal consequence of supercontinent aggregation and disaggregation suggests otherwise. Formation of a supercontinent elevates the T_P underneath the continents owing to heat transfer inefficiency of thick, stagnant continental lithosphere relative to thinner, subducting oceanic lithosphere (Coltice et al. 2009; Lenardic et al. 2011). Moreover, if a supercontinent is surrounded by subduction zones, to keep the average T_P constant, an increase in T_P beneath continent is accompanied by a drop in T_P beneath oceans. Lenardic et al. (2011) showed that the change in mantle thermal state would result from the insulating effect of continental lithosphere no longer being communicated to the suboceanic mantle via thermal mixing. Thus supercontinent formation and break-up in the Precambrian (Condie 2004) might have caused the mantle wedge

T_P, and hence the near-surface slab temperatures, to fluctuate. The implication for subduction of crustal carbonate is that recycling of carbon beyond sub-arc depths may be promoted during the stability of a supercontinent with lower mantle wedge potential temperatures. Supercontinent break-up, on the other hand, would lead to a transient burst of enhanced convective vigor driven by a strong lateral thermal gradient beneath continents and oceans and corresponding increases in the T_P of the mantle wedge. This change, in turn, would trigger breakdown of slab carbonates, causing massive CO_2 outgassing at arcs. However, slower plate velocity during this supercontinent stage may offset the effect of a cooler mantle wedge and may lead to warming of the slab-surface during subduction. This effect would then be more effective in triggering slab decarbonation. More work, using both rock records and geodynamic modeling, is needed to constrain the thermal structures of the Precambrian subduction zones through time, as there may be short-term oscillations from hot to moderately hot or relatively cold subductions, modulating the efficiency of carbonate recycling. This effect is particularly important because inefficient ingassing of CO_2 may have helped the planet to recover from hard snow-ball state as recent as Neoproterozoic (Kirschivink 1992).

Carbon ingassing in modern Earth

Recycling. A number of studies have discussed Earth's carbon cycle, taking into consideration the cycle involving the planet's interior relevant for the Phanerozoic Eon in general and that of modern Earth in particular (Kerrick 2001; Sleep and Zahnle 2001; Hayes and Waldbauer 2006; Dasgupta and Hirschmann 2010). Thus, here only the salient features of modern Earth's deep carbon ingassing via recycling of near-surface rocks are reviewed, highlighting the new observations and drawing attention to potential new directions of study.

Dasgupta and Hirschmann (2010) suggested that the total input of carbon into subduction zones is $(6.1\text{-}11.4) \times 10^{13}$ g of C/yr, which includes an oceanic mantle lithosphere contribution of 3.6×10^{13} g of C/yr (assuming ophicarbonates contain ~11 wt% CO_2 and the top 100 m of the mantle lithosphere is composed of a pervasive ophicarbonate layer). However, if this value is revised with bulk serpentinite content of only 500-1000 ppm C (Alt et al. 2012) and the estimate of serpentinite proportion as preferred by the same authors (Alt et al. 2012), mantle subduction does not contribute more than $(\sim 0.5\text{-}1.0) \times 10^{13}$ g C/yr. Thus the revised estimate of the present-day subduction input of carbon, combining all lithologies, becomes $(5.4\text{-}8.8) \times 10^{13}$ g C/yr. Although the global outgassing flux of carbon through intraplate volcanism is largely unconstrained, if such flux is small (given much smaller mass flux of intraplate volcanism), the present-day subduction input of carbon may be more than the outgassing flux combining ridges, hotspots, and arcs. With mantle inventory of carbon being the topic of interest, the obvious question then becomes that how much of this carbon goes past sub-arc depths of 72-173 km (Syracuse and Abers 2006) and thus likely participates in a much longer time scale cycle involving the deep mantle.

Similar to the Archean-Proterozoic times, carbon ingassing flux of the present-day mantle is also being shaped primarily by thermal vigor of the plate boundary processes, i.e., thermal structure of modern subduction zones. The preceding discussion and Figures 8 and 9 indicate that although carbon ingassing by crustal recycling likely was hindered by a hotter Earth in the Hadean Eon, in the Archean Eon and a significant portion of the Proterozoic Eon slab-surface temperatures likely became cooler than the average decarbonation and carbonate melting solidi temperatures by the Mesoproterozoic to Neoproterozoic era. Indeed, the comparison of *P-T* paths of downgoing slabs estimated for modern Earth subduction zones (van Keken et al. 2002; Syracuse et al. 2010) (Fig. 10), combined with petrologic constraints on carbonate/CO_2-bearing lithospheric assemblages, has prompted many investigators to conclude that at present-day carbon subducts deep into Earth with only minor outgassing via arc environments (Yaxley and Green 1994; Kerrick and Connolly 1998; Molina and Poli 2000; Kerrick 2001; Kerrick and Connolly 2001; Dasgupta et al. 2004; Dasgupta et al. 2005; Thomsen and Schmidt
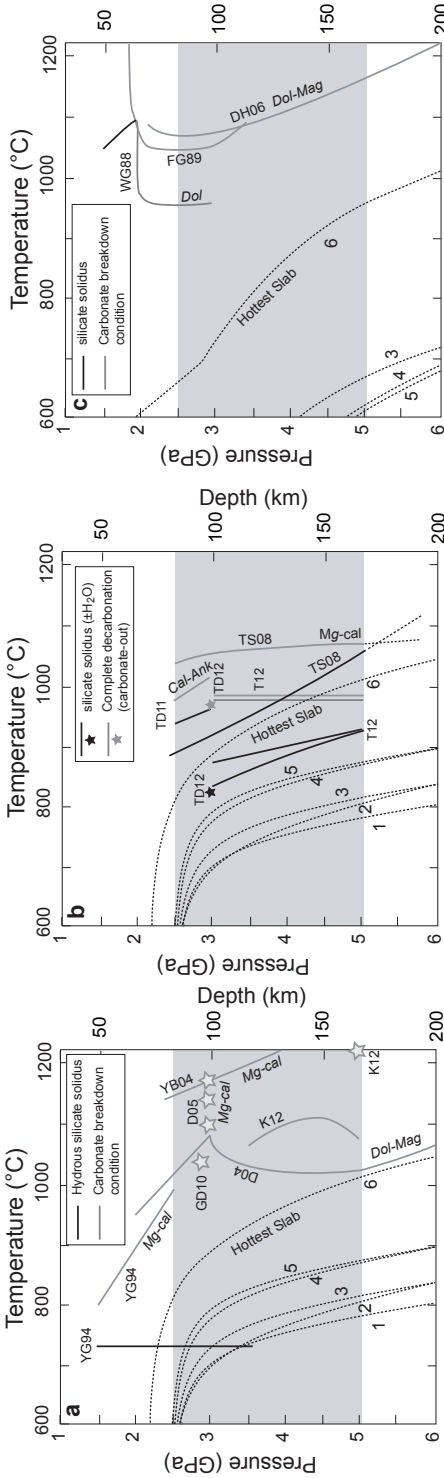
Figure 10. Subduction efficiency of carbon in present day Earth, based on the comparison of subducting slab *P-T* paths worldwide (Syracuse et al. 2010) and the available experimental boundaries of decarbonation and melting of carbonated basalt (a), carbonated pelite (b), and carbonated peridotite (c). Experiments that constrain the decarbonation and melting of subducting lithologies are the same as those plotted in Figure 8. The subducting slab *P-T* paths (dashed lines with numbers next to them) plotted in (a) and (b) are those for the top surface of the slabs, given that both sedimentary and secondary carbonates in oceanic basalt reside mostly within top 500 m of the slab. The subducting slab *P-T* paths in (c) are those for the base of the 7 km thick oceanic crust or at the top surface of the mantle lithosphere. The slab-surface *P-T* paths in (b), marked with 1 through 5, are specifically for those subduction zones where ocean-floor sediments are known to have a distinct carbonate fraction (Plank and Langmuir 1998). The gray shaded region marks the range of sub-arc depths for all modern subduction zones combined (Syracuse and Abers 2006). Carbonate mineral major element compositions stable along the phase boundaries are marked (see legend to the left). Lithologies that stabilize dolomite solid solution or dolomite-magnesite solid solution on average have lower carbonate-out boundaries compared to those that stabilize calcitic solid solution.

Subducting slab P-T conditions

1 - Sunda   2 - Antilles   3 - South Vanuatu
4 - Nicaragua   5 - North Vanuatu   6 - North Cascadia

Hottest slab - slab-top trajectory for Cascadia

   Sub-arc depth range

Carbonate mineral abbreviations

Mg-cal - magnesian calcite solid solution
Dol-Mag - Dolomite-magnesite solid solution
Cal-Ank - Calcite-ankerite solid solution

2008; Dasgupta and Hirschmann 2010; Tsuno and Dasgupta 2011; Tsuno and Dasgupta 2012). If this is the case then a significant portion of the original input of $(5.4\text{-}8.8) \times 10^{13}$ g C/yr could be recycled deep into the mantle. However, the arc flux of CO_2 [$(1.8\text{-}3.7) \times 10^{13}$ g C/yr; (Sano and Williams 1996)] demands that up to ~20-70% of the original carbon input to subduction zones be returned to the atmosphere by arc magmatism. In addition, fluxes associated with metamorphic and hydrothermal fluids not generally included in volcanic flux estimate may call for even greater extent of CO_2 transport from slab to the surface. Furthermore, the proposition that primary arc magmas might be more CO_2-rich than previously thought (Blundy et al. 2010) and intrusives associated with arc volcanos may also contain carbon, suggest that arc flux of CO_2 may be larger than previously estimated. Thus, there is an apparent contradiction between the petrologic prediction of carbonate stability in the subducting slab and measured flux of carbon in arc volcanic centers. The following are some of the processes that can potentially explain this paradox.

1. A significant decarbonation of crustal carbonates (in altered basalt and in sediments) may take place by influx of water derived from extraneous sources, such as underlying serpentinite sections (Gorman et al. 2006). The chief uncertainty in this process is pervasiveness of the fluid flushing through basaltic crust and sediment at sub-arc depths. If serpentinized zones are created via bending faults in the outer rise, then serpentinites may be spatially restricted (Ranero et al. 2003) and thus fluids liberated from them may not flush through the overlying crust pervasively but remain in channels. In such a scenario, decarbonation may not be significant.

2. The hydrated top portions of the subducting slab, including sediments, basaltic crust, and mantle lithospheric section, may detach from the downgoing slab and rise to wedge mantle as Rayleigh-Taylor instabilities (e.g., Gerya and Yuen 2003; Castro and Gerya 2008). If this happens then slab carbonates may experience hotter wedge temperature, thereby undergoing melting or decarbonation and releasing CO_2.

3. Owing to density contrast alone and not aided by hydration, downgoing sedimentary packages may undergo diapiric rise into the mantle wedge (Currie et al. 2007; Behn et al. 2011). Signature of sediment partial melt and sedimentary carbon in arc volcanics thus may be derived by sediment decarbonation and melting in the mantle wedge, as proposed by the studies of Tsuno and Dasgupta (2011, 2012), Tsuno et al. (2012), and Behn and co-workers (2011).

4. Based on fluid inclusions trapped in diamonds of ultra-high pressure rocks of Western Alps that preserved dissolved bicarbonate and carbonate ions and crystals of carbonate in the inclusions, it has been suggested that the transfer of carbon from slab to wedge takes place by carbonate dissolution in the fluid at sub-arc depths, rather than by decarbonation or melting (Frezzotti et al. 2011).

5. A sizeable portion of the global arc flux may derive from metamorphic decarbonation of crustal carbonates in the overriding plate through interaction with arc magmas. For example, Mount Etna [1.3×10^{13} g CO_2; (Allard et al. 1991)] and Vesuvius, which erupt through thick sections of crustal carbonates, make up 20% of the global CO_2 arc out flux. The presence of skarn xenoliths and heavy carbon isotope chemistry of fumarolic gases in Mt. Etna and Vesuvius do suggest sedimentary carbonate assimilation at arc crust (e.g., Iacono-Marziano et al. 2009). Although this non-mantle CO_2 outflux tends to be more important at old continental arcs, owing to the possible presence of crustal carbonates, even in the juvenile continental crust this contribution could be more than previously recognized. If global arc CO_2 flux is increased significantly by this form of crustal carbonates in the overriding plate, then one important corollary would be that a greater percentage of trench input of carbon actually gets recycled deep into the mantle.

The relative contributions of these various mechanisms to the outgassing flux of carbon in modern subduction zones are unconstrained at present. Also unconstrained is how much CO_2 can be carried in siliceous hydrous partial melts of sediments, which appears to be a an unavoidable agent of mass transfer in subduction zones. With all recent estimates of slab-surface temperatures being hotter than the fluid-present solidi of subducting crust and sediments (van Keken et al. 2002; Syracuse et al. 2010; Cooper et al. 2012) and the flux of hydrous fluid perhaps being available from breakdown of hydrous phases in subjacent lithologies (e.g., serpentinites), it becomes critical to know the carrying capacity of CO_2 in high-pressure hydrous siliceous melts (Ni and Keppler 2013).

Acquisition of mantle carbon via interaction of subducted 'water' and metallic core? All possible processes for explaining the "excess" carbon in the mantle paradox that were discussed before are early Earth processes that could have restored the mantle carbon budget well before the initiation of plate-tectonics. However, as suggested by Dasgupta et al. (2013a), the initiation of plate tectonic cycles may have provided another pathway for elevating mantle carbon over geologic time, i.e., in addition to introducing surficial carbon by recycling. They proposed that if subduction of oceanic plate brings water to the core-mantle boundary (CMB) regions, it may be possible that water, expelled from breakdown of hydrous phases or contained in hydrous phases, reacts with metallic alloy melt from outer core to form Fe-hydrides, FeH_x (Okuchi 1997; Okuchi 1998; Terasaki et al. 2012); Fig. 5d). Oxygen, being less soluble in the metallic core and released in the process, then may react with carbon in the core to form CO_2, CO, or $FeCO_3$, following a set of reactions such as:

$$Fe + H_2O = FeO + 2H \tag{11}$$

$$Fe + xH = FeH_x \tag{12}$$

$$FeO + C = Fe + CO \tag{13}$$

$$2FeO + C = 2Fe + CO_2 \tag{14}$$

$$FeO + CO_2 = FeCO_3 \tag{15}$$

Excess hydrogen, not dissolved in the metallic core, may also react with carbon to release hydrogenated species such as methane, following the reaction:

$$C + 2H_2 = CH_4 \tag{16}$$
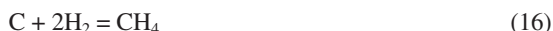
It is also possible that such reaction stabilizes other multi-light element alloys, such as $FeSiH_x$ (Terasaki et al. 2011), following the reaction such:

$$FeSi + xH = FeSiH_x \tag{17}$$

The produced CO, CO_2, hydrocarbons, or carbonate most likely forms a component in a melt phase in D″. Such C-bearing melt may be released from the core, eventually causing the mantle carbon concentration to increase. Similar to the model of inefficient core formation, this possibility could also make the lower mantle more carbon-rich. One caveat to this speculation is that while the reaction with subducted hydrous phases and the core may release carbon to the mantle, if a subducted slab carries carbon down to the CMB regions, then subducted carbon may also be lost to core. Therefore, if both recycling and core-slab interactions contribute to modern Earth's mantle carbon budget, then slabs in the CMB graveyard need to be hydrous but carbon-poor.

Carbon in modern Earth's mantle: recycled versus primordial? With deep carbonate subduction being quite efficient at least over the Phanerozoic Eon, and maybe for the past 1 billion year, one may wonder whether the present-day inventory of mantle carbon is chiefly recycled or primordial. For example, if mantle outgassing rate at oceanic ridges is controlled by deep carbonated melting at a depth exceeding 300 km (Dasgupta and Hirschmann 2006),

then the residence time of mantle carbon can be as short as 1 Ga, thus requiring a significant fraction of the present-day mantle carbon to be recycled. Whereas if redox freezing (as graphite, diamond, C-bearing metal alloy, or metal carbide) suppresses deep melting-induced efficient liberation of carbon, then the residence time of carbon in the mantle may approach 4 Ga, requiring limited input from Phanerozoic subduction to make up its inventory.

Carbon isotopic composition of mantle-derived samples shed light on the possible origin of present-day mantle carbon. The average value of $\delta^{13}C$ of mantle carbon is ~ −5 (Deines 2002), with more negative excursions [i.e., carbon that is isotopically lighter, up to −25‰; (Stachel et al. 2005)] typically associated with graphite and diamonds (e.g., Schulze et al. 1997; Walter et al. 2011). Although the origin of "light" carbon in the mantle is debated (Cartigny 2005), a leading hypothesis is that the light mantle carbon ($\delta^{13}C < -10‰$) results from subduction of the isotopically light organic carbon fraction of altered oceanic crust, sediments, or mantle lithosphere (Stachel et al. 2005). However, it still remains an unsolved mystery why most of the mantle carbon presents $\delta^{13}C$ ~ −5‰, given that the dominant mass flux of carbon via carbonate subduction injects $\delta^{13}C$ ~ −1‰ (Coltice et al. 2004; Stachel et al. 2005). In particular, in the context of ancient versus modern processes shaping the carbon chemistry of the mantle as discussed in this chapter, the study of Satish-Kumar et al. (2011) re-opens the debate on the origin of the carbon isotope compositional variability of the mantle. Satish-Kumar and co-workers (2011) presented experimental evidence of carbon isotope fractionation between Fe-carbide melt (C-saturated metallic-Fe melt) and graphite/diamond and showed that Fe-carbide melt prefers isotopically light, ^{12}C-enriched carbon over graphite/diamond. Although it remains unclear whether Earth's early magma ocean was graphite-saturated and whether the C-isotope fractionation between silicate magma ocean and C-poor metal melt would yield a similar ^{12}C-enriched core melt, it is plausible that carbon derived from metallic melt generates in part the light isotopic signature observed in many deep diamonds. Therefore, if inefficient core formation leaves behind a small fraction of C-bearing metallic melt, such phases may contribute towards the carbon isotopic heterogeneity of mantle samples and in particular may provide the light carbon in the mantle. Furthermore, carbon isotopic fractionation between metal and silicate melts might have established the $\delta^{13}C$ near the average mantle value of −5‰ and potentially explain the difference between CI chondrites ($\delta^{13}C$ −7 to −15‰) (Kerridge 1985) and that of Earth's mantle.

Break-up of Pangea and perturbation of the Phanerozoic deep carbon cycle. Although present-day estimates of slab thermal profiles suggest only a limited decarbonation of downgoing lithosphere at sub-arc depths, any increase in arc mantle potential temperatures would disrupt such balance of deep carbon cycling and force carbon to be released at sub-arc depths and thus outgassed by arc volcanism. Were there any time periods in the Phanerozoic Eon when the subduction zones could have become hotter? Formation and break-up of supercontinent Pangea might have created such a scenario. Thermal mixing in the mantle soon after the supercontinent break-up could have caused the arc source mantle to heat-up by as much as 200 °C (Lenardic et al. 2011). As a consequence, the slab surface temperatures beneath arcs might have increased by ~100 °C. With such a change in slab temperatures within a short period of time, carbonate melting and decarbonation of subducting crusts are expected and cause shut-down of the deep carbon influx for perhaps a few tens of million years. Very short residence times of subducted carbon and release through arc volcanism thus might have played a critical role in the Cretaceous and early Paleogene (~140-50 Ma) greenhouse climate. Greater abundance of continental arcs over island arcs at this time period (Lee et al. 2013) might have also caused excess CO_2 to be released through metamorphic decarbonation and assimilation of sedimentary carbonates in the arc crust as observed in Mt Vesuvius and Etna of modern Earth (Iacono Marziano et al. 2008; Iacono-Marziano et al. 2009; Lee et al. 2013).

Stable forms of carbon in the modern mantle and carbon outgassing

With deep ingassing appearing to be efficient for most part of the last ~1.5 Ga, the question becomes what are the stable forms of carbon in Earth's modern mantle (Oganov et al. 2013)? Moreover, how do the stable hosts of carbon vary as a function of depth and various tectonic settings? Again, a number of studies reviewed the mineralogic and petrologic constraints on carbon storage in the mantle (Luth 1999; Dasgupta and Hirschmann 2010), thus this section is aimed at highlighting only some of the new insights based on recent experimental observations.

Carbonated melt in the convecting oceanic mantle. Owing to very limited solubility of carbon in the silicate minerals of Earth's mantle (Keppler et al. 2003; Shcheka et al. 2006), carbon's presence in the mantle is controlled chiefly by the thermodynamic stability of various C-bearing accessory phases and dynamic and thermodynamic stability of C-bearing fluids and melts. In shallow oceanic mantle beneath ridges, oxidized form of carbon exists and carbonated melt—either carbonatite or carbonated silicate melt (Dalton and Presnall 1998; Gudfinnsson and Presnall 2005; Dasgupta and Hirschmann 2006; Dasgupta et al. 2007a, 2013b)—could dominate the budget of mantle carbon to ~300 km (Fig. 7). However, it is also plausible that carbonated melts freeze by a redox process at the expense of diamond/graphite (e.g., Eqns. 7 and 8) at depths shallower than ~300 km (the depth of intersection of carbonated peridotite solidus and the mantle adiabat of T_P ~1350 °C) (Stagno and Frost 2010; Rohrbach and Schmidt 2011; Dasgupta et al. 2013b). The depth of reduction of carbonated melt to diamond/graphite is debated at present. Stagno and Frost (2010) suggest such destabilization of carbonated melt as shallow as 100-150 km, whereas the study of Rohrbach and Schmidt (2011) places this depth to ~250 km (Fig. 6), based on the experimental observation that majorite (significant host of Fe^{3+}) becomes stable at such a depth and saturation of Fe-Ni alloy is achieved (Rohrbach et al. 2007; Rohrbach et al. 2011). The carbon release depth of 300 km (by carbonated melting) versus as shallow as ~100-150 km (by redox melting) must have critical difference for the outgassing rate of carbon in the modern mantle. For example, Dasgupta et al. (2013b) showed that with redox transformation of carbonate to diamond at ~250 km depth, the first melt in the upwelling mantle globally will be a carbonated silicate melt of kimberlitic affinity rather than carbonatite *sensu stricto*. This conclusion rests on the experimental observation that carbonate-silicate melt mixing is favored at greater depth and hence the stability field of carbonated silicate melt expands over the field of true carbonatite. Dasgupta et al. (2013b) argued that if the depth-oxygen fugacity evolution is taken into account, carbonated silicate melt with 15-25 wt% CO_2 and modest amount of water is likely a more important agent releasing incompatible trace elements and fluids to the exosphere.

Even though carbonate melt/mineral stability may be compromised at the face of iron disproportionation-induced redox freezing, locally carbonate-rich regions (perhaps regions that are affected by subduction of carbonates) may persist to even lower mantle depths (Biellmann et al. 1993; Stagno et al. 2011). In such a scenario the topology of carbonated peridotite solidus could apply to the entire depth range plotted in Figure 7, i.e., through mantle transition zone to lower mantle. Experimental determination of the solidus slope of carbonated peridotite at transition zone and lower mantle depths, combined with the knowledge of the same in the upper mantle, suggests possibly an interesting case of carbonatite generation in the deep mantle. Figure 7 shows that if a mantle adiabat for T_P of 1350 °C is followed, then there could be a "double-crossing" of the carbonated peridotite solidus, one at ~10 GPa and another at ~30 GPa. The exact depth of the latter intersection remains somewhat uncertain owing to lack of experimental constraints on the solidus for relevant compositions at >25 GPa. However, the key point is that the "double-crossing" of the adiabat and the solidus suggests that carbonatite generation not only can take place at ~300 km depth by adiabatic decompression of the mantle, but also at lower mantle depth of ~800-900 km by compression or convective down-welling of the mantle transition zone materials. A corollary of the solidus-adiabat double-crossing is

that a large fraction of the transition zone may be below the carbonatite solidus and thus may have carbon stored as magnesite, provided the oxygen fugacity is >IW+2 (Stagno et al. 2011). Thus, trace carbonatite melt may affect the seismic structure of the deep upper mantle and also shallow lower mantle but perhaps not the mantle transition zone.

Carbon and carbonates in the continental lithospheric mantle. While oxidized form of carbon in asthenospheric upper mantle is chiefly a melt phase, continental lithospheric mantle can contain stable crystalline carbonates. Figure 11 shows that in the shallow continental lithospheric mantle to a depth of ~100-220 km (geotherms corresponding to surface heat flux of 40-50 mW m^{-2}), carbon can exist as crystalline carbonate, i.e., magnesite and dolomite solid solution (Fig. 11) and only at greater depths do the continental shield geotherms cross the carbonated peridotite solidus and hence magnesio-carbonatite melt (Dasgupta and Hirschmann 2007b) becomes stable in the lithospheric mantle. If the carbonated peridotite domain is also hydrous and amphibole-bearing, then the solidus can be slightly lower (Wallace and Green 1988) and magnesite/dolomite may be restricted to slightly shallower depths. Although carbonatitic melt may be stable at depths deeper than 100-220 km, diminishing oxygen fugacity with depth, as recorded in the Fe^{3+}/ΣFe of garnets in cratonic mantle xenoliths and determined based on the oxy-thermobarometry calibration of Gudmundsson and Wood (1995), suggests that graphite/diamond may become stable over crystalline carbonate or carbonated melt at 100-150 km depth (Woodland and Koch 2003; McCammon and Kopylova 2004; Stagno and Frost 2010; Yaxley et al. 2012). If this is the case, then the stability of primary carbonatitic melt in Archean cratonic environments may be restricted within a narrow window of ~1050-1100 °C
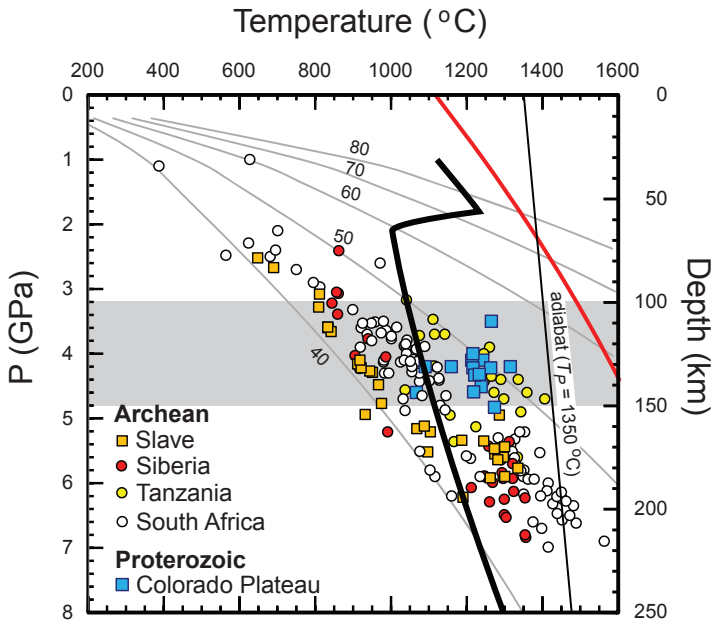

Figure 11. Comparison of carbonated fertile peridotite solidus (thick black line) from Figure 6 with geotherms based on xenoliths of the Archean and Proterozoic cratonic peridotite. Steady-state conductive geotherms are for a surface heat flux of 40-80 mW m^{-2}. Shown for reference are volatile-free peridotite solidus (red line) from Hirschmann (2000) and proposed depth range of carbonate to graphite/diamond transition (gray horizontal band; (Stagno and Frost 2010; Yaxley et al. 2012) based on skiagite activity in garnet and experimental oxy-barometry calibration of Gudmundsson and Wood (1995). The xenolith geotherm data are from Lee et al. (2011).

and 100-150 km. Somewhat deeper production of carbonated melt in the cratons is possible, however, with metasomatically oxidized and more carbon-rich domains, either through redox or carbonated melting (e.g., Foley 2008). Although carbonate melting may be restricted for greater thickness of thermal boundary layer in the Archean cratons, elevated geotherms similar to those of the Proterozoic (surface heat flux of ~50 mW m^{-2}) and Phanerozoic terrains (surface heat flux of >60-80 mW m^{-2}) would stabilize carbonatitic melt as shallow as 70-100 km (Fig. 11), depths at which conversion from carbonate to graphite likely does not occur.

   Deep storage of carbon — deep upper mantle to lower mantle. Although oxidized phases such as CO_2-rich fluid, carbonatite, and carbonated silicate melt are the chief hosts of carbon in the shallow (< 200-250 km) upper mantle, the dominant storage mechanism of carbon changes at greater depths. In a mantle poor in carbon, and thus oxygen fugacity being controlled by the Fe^{2+}-Fe^{3+} exchange and energetics of Fe^{3+} incorporation in mantle silicates, mantle likely becomes metal-saturated as shallow as 250±30 km and remains such at greater depths (Frost and McCammon 2008; Rohrbach et al. 2011). A consequence of this environment is the equilibrium reaction of carbon with Fe-Ni metal and mantle storage of the former in Fe-rich alloy, Fe-rich carbides, and as diamond (Frost and McCammon 2008; Dasgupta and Hirschmann 2010; Buono et al. submitted). Albeit rare, natural inclusions of Fe-carbide, Fe_3C and metallic-Fe in mantle-derived diamonds (Sharp 1966; Jacob et al. 2004; Kaminsky and Wirth 2011) validate such experimental predictions. But what further experimental constraints can be provided in terms of the relative roles of alloy versus carbides versus diamond versus metallic liquid as the host of deep carbon? The exact phase of interest that hosts carbon depends on the bulk composition in the Fe-C (±Ni ±S) system, and the *P-T* condition in question. The concentration of Fe-Ni metal is predicted to vary between 0.1 and 1.0 wt% with ~0.1 wt% metal alloy being stable from the deep upper mantle through the transition zone and ~1 wt% metal alloy being stable almost throughout the lower mantle. The alloy composition is also predicted to vary from 39 wt% Fe - 61 wt% Ni at ~250 km depth and 88 wt% Fe - 12 wt% Ni at the lower mantle (Frost and McCammon 2008). The current knowledge of the effect of Ni on the high-pressure phase relations in the Fe-C system is limited thus the prediction from Fe-C binary phase diagrams are discussed first. In Figure 12, the estimated Fe-C phase diagrams at pressures of 10 and 50 GPa from the study of Lord et al. (2009) are presented and compared with the mantle temperatures expected at such depths. The key observation from Figures 12a and 12b are: (a) at the base of the upper mantle and for an average MORB source carbon content not exceeding 30 ppm C (equivalent of 110 ppm CO_2) all the carbon will be dissolved in an alloy ± a metallic melt phase; (b) for cohenite to be a phase of interest, the deep upper mantle needs to contain carbon in excess of ~50 ppm; and (c) for diamond to be an equilibrium phase, carbon content in excess of ~90 ppm is needed. Although the detailed phase diagram of the Fe-Ni-C system as a function of pressure is not well constrained, recent experimental work at 3 and 6 GPa suggests that Ni behaves as an incompatible element in the cohenite-Fe-Ni-C(±S) liquid system (Buono et al. submitted), suggesting that Ni does not stabilize cohenite and Ni lowers the melting point of cohenite. Hence, it is expected that if the metal is Ni-rich at the base of the upper mantle and throughout the transition zone then the Fe-Ni-C melt will be a more dominant carbon host than predicted from the Fe-C phase diagram alone. Moreover, as sulfur in the mantle is present almost entirely as sulfides—given the oxygen fugacity of the mantle (e.g., Jugo et al. 2010)— equilibrium phase relations and geochemistry of the Fe-(±Ni)-C-S system also become relevant to constrain the equilibrium carbon-bearing phase. Sulfide-metal-metal carbide connection in the mantle is also evident from common association of pyrrhotite or troilite with iron carbide and Fe-rich metal alloy phases in inclusions in diamonds (Sharp 1966; Jacob et al. 2004). In Figure 13, the plausible range of Fe-(±Ni)-C-S composition relevant for the mantle subsystem is shown. Also shown are the available near-liquidus phase relations for Fe-Ni-C-S, Fe-Ni-C, and Fe-C-S bulk compositions over the pressure range of 3 to 6 GPa (Dasgupta et al. 2009a; Buono et al. submitted). It can be observed, with reasonable extrapolation of the experimental
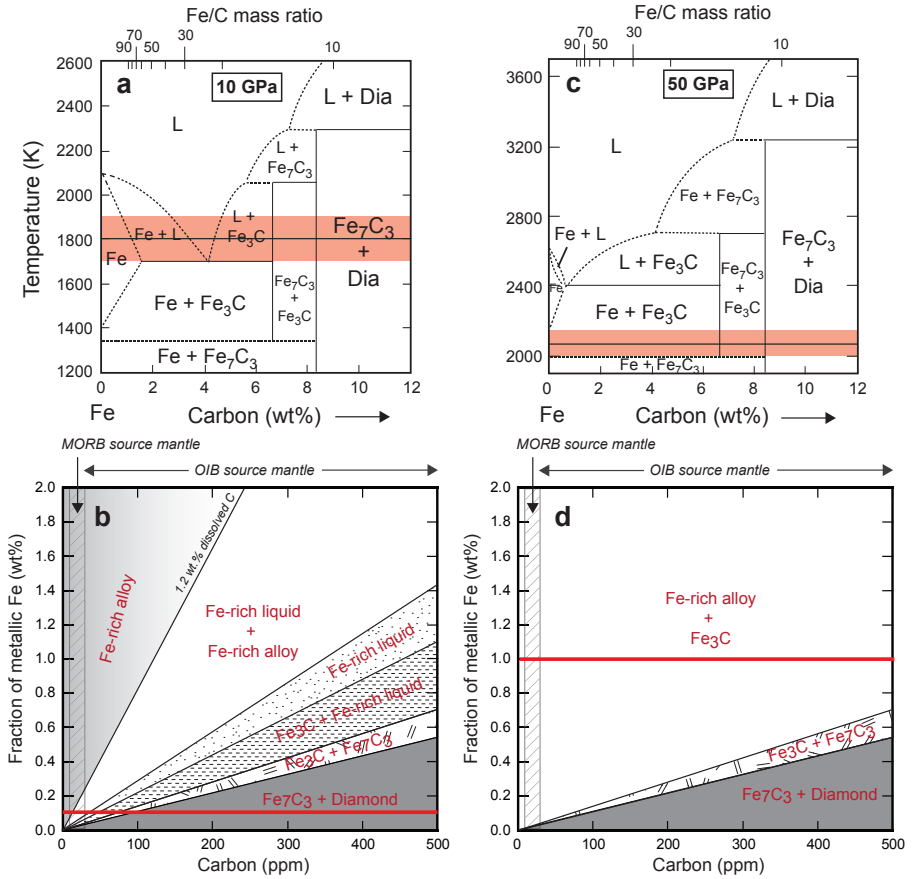
Figure 12. Iron-rich portion of the Fe-C binary phase diagrams at (a) 10 GPa and (c) 50 GPa adapted from the study of Lord et al. (2009). Also marked along the top *x*-axis are the Fe/C mass ratios for various bulk compositions. The shaded band with lines in the middle in (a) and (c) indicate the expected temperatures of the mantle along an average mantle adiabat derived from Brown and Shakland (1981) at these depths. (b) and (d), based on the phase diagram (a) and (c) respectively, show the expected phase assemblages in Fe-Ni metal alloy in the mantle (in weight percent) and carbon content (in ppm) of the mantle space. (b) and (d) thus present the expected reduced carbon-bearing phases in the deep upper mantle and lower mantle, respectively, as a function of metallic alloy and carbon content. The red horizontal lines in (b) and (d) mark the expected mass fraction of alloy at these mantle depths as suggested by Frost and McCammon (2008). Reduced solubilities of carbon in carbide-saturated alloy at higher pressures suggest that carbide-saturation of the mantle takes place even for a carbon depleted MORB-source mantle at lower mantle depths, whereas for a similarly carbon-poor deep upper mantle, the entire carbon inventory could be dissolved in a metallic alloy phase (see text for details). The plot in (d) also suggests that unless a small amount of Ni has a large influence on the Fe-C phase diagram, diamond stability in the lower mantle requires the mantle to be extremely carbon-rich or much poorer in metal alloy fraction.

phase boundaries, that the sub-ridge adiabatic temperatures may yield an Fe-Ni-C-S melt at depth of first metal saturation, i.e., 250 ± 30 km. If the mantle adiabatic gradient relevant for intraplate ocean island sources is considered then Fe-Ni-C or Fe-Ni-C-S melt will likely be stable throughout the deep upper mantle, possibly even throughout the transition zone. Furthermore, although carbon-bearing Fe-Ni-S melt likely is stable in the deep upper mantle and transition zone, the involvement of sulfur may help and be necessary for stabilizing diamond at these
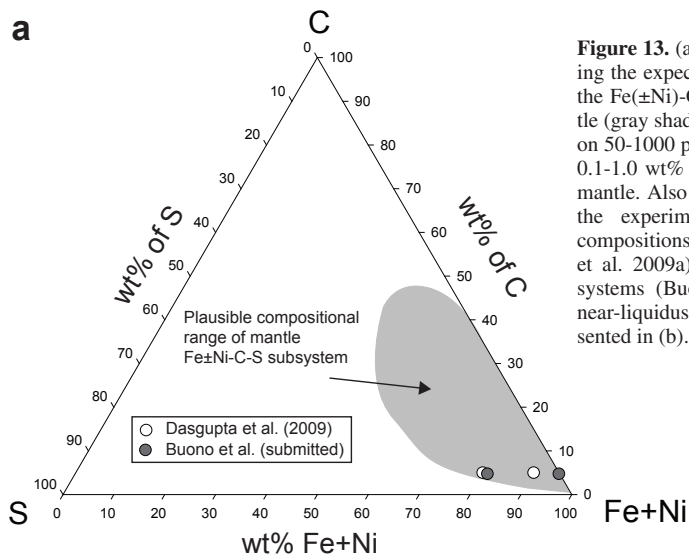
Figure 13. (a) Fe+Ni-C-S ternary showing the expected compositional range in the Fe(±Ni)-C-S subsystem of the mantle (gray shaded field). The field is based on 50-1000 ppm C, 150-350 ppm S, and 0.1-1.0 wt% Fe-Ni alloy fraction in the mantle. Also shown for comparison are the experimentally investigated bulk compositions in the Fe-C-S (Dasgupta et al. 2009a), Fe-Ni-C, and Fe-Ni-C-S systems (Buono et al. submitted), the near-liquidus relations for which are presented in (b).
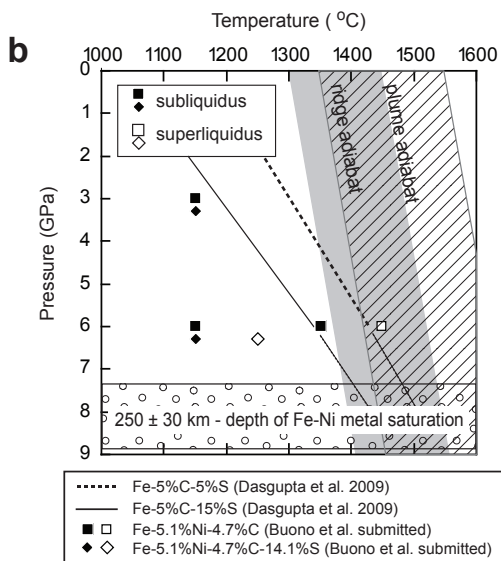
(b) *P-T* diagram showing the experimental constraints on the liquidus of Fe-C-S (Dasgupta et al. 2009a) and Fe-Ni-C±S (Buono et al. submitted) bulk compositions shown in (a). Shown for comparison in (b) are the mantle adiabats relevant for MORB and OIB production, i.e., ridge adiabat and plume adiabat, respectively. Also shown for reference is the minimum depth where Fe-Ni alloy saturation is thought to occur according to the study of Rohrbach et al. (2011). Comparison between the liquidi of the metallic compositions and the adiabats suggests that, especially for S-bearing and S-rich compositions, the deep upper mantle may contain a sulfide-rich Fe-Ni-C-S metallic liquid phase and solid carbide stability may require somewhat greater, perhaps transition zone depths.

depths. Owing to strong non-ideality of mixing in the Fe-(±Ni)-C-S systems (Wang et al. 1991; Corgne et al. 2008; Dasgupta et al. 2009a), S-rich Fe-Ni-S melt may repel carbon and force diamond saturation. Data available in Fe-Ni-C-S systems suggest that diamond nucleation may be aided by the presence of a Fe-Ni sulfide melt (Shushkanova and Litvin 2008; Zhimulev et al. 2012) because C-solubility in Fe-alloy melt is known to diminish with increasing sulfur content (Ohtani and Nishizawa 1986; Tsymbulov and Tsmekhman 2001; Zhimulev et al. 2012). Thus, although Figure 12 suggests that deep upper mantle diamond only forms from a C-rich (>100 ppm C or ~370 ppm CO_2) mantle, S-rich systems may lead to diamond formation at lower C content. However, more work on sulfide-metal-carbide system is necessary to constrain the relative contributions to various C-bearing phases in detail.

The scenario of carbon storage in the lower mantle could be different (Fig. 12c,d). This expected change is aided by the following. (1) The metal content in the lower mantle can be as much as 1 wt% (Frost and McCammon 2008) and hence, unless the lower mantle is more carbon-rich compared to the deep upper mantle, the effective Fe/C ratios of the metal subsystem become higher. (2) The composition of the metal phase is Fe-rich and Ni-poor, hence the Fe-C binary exerts more control on the mode carbon storage. (3) The solubility of C in carbide-saturated metallic alloy is expected to diminish strongly as a function of pressure (Lord et al. 2009; Walker et al. accepted). The estimated rate of movement of the Fe-C eutectic as a function of P to C-poor compositions suggests that the C-solubility in metal alloy may become negligible by 50 GPa (Fig. 12c; Lord et al. 2009). A consequence of all of these observations is that a vast region of lower mantle may display coexistence of cohenite and Fe-rich metallic alloy for Fe/C ratios relevant for both MORB and ocean island basalt source regions. This assemblage is distinct from the mode of carbon storage in metallic systems at upper mantle and transition zone depths, where carbide may not be a stable phase for carbon-poor MORB source compositions (≤ 110 ppm CO_2). It can also be noted in Figure 12d that, if the lower mantle contains ~1 wt% Fe-rich metal alloy, then in an equilibrium scenario the stability of diamond and Fe_7C_3 is unexpected unless the mantle domains are extremely carbon-rich (>700-1000 ppm C). More experimental work in the Fe-Ni-C-S system at lower mantle depths will be needed to refine these predictions and gain further insight into deep mantle carbon storage in reduced phases.

CONCLUDING REMARKS

In response to the evolving thermal vigor and fugacity of oxygen and other volatiles, the behavior and fate of carbon and its partitioning between various layers of Earth (atmosphere, silicate Earth, and metallic core) varied through geologic time. During the first few tens of millions of years of the Hadean Eon, carbon that was not lost to space and participated in the core-forming magma ocean processes appears to have partitioned strongly into the metallic core. This fractionation would have made core the largest terrestrial reservoir of carbon. However, uncertainty in the core carbon budget remains owing to poor constraints on bulk Earth carbon in a magma ocean environment, the lack of consensus on the extent of metal-silicate equilibration, the composition of the impactors (including the composition of the core of the differentiated impactors), and the lack of availability of experimental data on partition coefficient of carbon in a deep, reduced magma ocean environment, involving a multi-component metallic alloy melt. With almost all carbon of the chondritic building blocks being lost to space, restricted to nascent atmosphere, or sunk to the core, the silicate liquid mantle soon after core segregation was probably carbon-poor. Processes such as late bombardment of volatile-rich material, entrapped C-bearing metallic liquid in the pore spaces of lower mantle solids, and ingassing from a C-rich atmosphere had opportunities to replenish mantle carbon by the end of the Hadean Eon. In fact, the mantle may have even attained carbon concentrations higher than that sampled by present-day oceanic volcanism at the end of the Hadean Eon. Greater thermal vigor of convection in the Archean Eon likely caused deeper and greater volume of carbonated melt generation and thus efficient outgassing of carbon ensued. The thermal state of the crustal recycling zone also likely was hotter until ~1.5 Ga; such slab thermal structure along with inconsistent subduction cycle likely hindered deep ingassing of surficial carbon. Massive release of CO_2 at Archean and Paleoproterozoic volcanic arcs thus may have supplied the necessary dose of greenhouse gas in the atmosphere to offset the dimmer early Sun and help sustain liquid water on Earth's surface. With secular cooling of Earth's mantle, the global systematics of ingassing and outgassing appear to have changed by the Meso- to Neoproterozoic Eras. The depth-temperature paths of subduction zones became amenable to transport of crustal carbonates past arc-magmatic processing depth, setting up systematic deep ingassing of carbon. A possible short-term

disruption of carbon ingassing and outgassing pattern may be caused by the mantle thermal state, owing to formation and break-up of supercontinents.

It remains unclear how the subducted carbon over the past 1-2 billion years distributed itself in the mantle, but with subduction going past the mantle transition zone, it is not unlikely that subducted carbon of the Proterozoic and Phanerozoic Eons is somewhat concentrated in the transition zone and lower mantle. It has also been speculated that deeply subducted water, carried in hydrous phases, may react with outer core alloy melt to trigger release of some core carbon. While ingassing of crustal carbon appear efficient in modern Earth, the petrology and dynamics of subduction zone processes including formation of sediment diapirs and fluid fluxed hydrous melting need to be closely evaluated to reconcile the modern arc flux of CO_2. With cycling of carbonates deep into the modern mantle globally, the storage mechanisms at depth becomes a key issue. Carbonate minerals and carbonatitic melt are stable at the shallow part of continental lithospheric mantle, while carbonated silicate melts are stable at the asthenospheric mantle. In subduction-influenced, carbon-rich, oxidized domains, carbonatitic melt may even be stable at the deep upper mantle through the top of the lower mantle. However, oxidized forms of carbon at depths greater than the deep upper mantle may be an exception and reduced phases such as Fe-Ni-S-C melt, Fe-Ni alloy, and Fe-rich carbides are the phases of interest with increasing depth, while diamond becomes a stable phase only in C-rich and/or S-rich mantle domains. Further work in multi-component metallic system will be required to understand the full spectrum of reduced carbon storage in the mantle. It also needs to be explored whether there are remnants of metallic alloy/carbide melt left behind from the event of core formation and whether such phases preserve very different compositions than those expected from iron disproportionation in silicates and subsequent alloy-C reaction.

ACKNOWLEDGMENTS

REFERENCES

Abe Y (1997) Thermal and chemical evolution of the terrestrial magma ocean. Phys Earth Planet Inter 100(1-4):27-39, doi: 10.1016/S0031-9201(96)03229-3

Alard O, Griffin WL, Lorand JP, Jackson SE, O'Reilly SY (2000) Non-chondritic distribution of the highly siderophile elements in mantle sulphides. Nature 407(6806):891-894

Albarede F (2009) Volatile accretion history of the terrestrial planets and dynamic implications. Nature 461(7268):1227-1233

Allard P, Carbonnelle J, Dajlevic D, Bronec JL, Morel P, Robe MC, Maurenas JM, Faivre-Pierret R, Martin D, Sabroux JC, Zettwoog P (1991) Eruptive and diffuse emissions of CO_2 from Mount Etna. Nature 351(6325):387-391, doi: 10.1038/351387a0

Alt JC (2004) Alteration of the upper oceanic crust: mineralogy, chemistry, and processes. *In*: Hydrogeology of the Oceanic Lithosphere. Vol. Davis EE, Elderfield H (eds) Cambridge University Press, p 497-535

Alt JC, Garrido CJ, Shanks Iii WC, Turchyn A, Padrón-Navarta JA, López Sánchez-Vizcaíno V, Gómez Pugnaire MT, Marchesi C (2012) Recycling of water, carbon, and sulfur during subduction of serpentinites: A stable isotope study of Cerro del Almirez, Spain. Earth Planet Sci Lett 327-328(0):50-60, doi: 10.1016/j.epsl.2012.01.029

Alt JC, Teagle DAH (1999) The uptake of carbon during alteration of ocean crust. Geochim Cosmochim Acta 63:1527-1535

Anders E, Grevesse N (1989) Abundances of the elements: meteoritic and solar. Geochim Cosmochim Acta 53:197-214

Ardia P, Withers AC, Hirschmann MM (2011) Methane solubility under reduced conditions in a haplobasaltic liquid. *In:* 42nd Lunar and Planetary Science Conference, Woodlands, Texas, USA. LPI Contribution No. 1608, p. 1659

Behn MD, Kelemen PB, Hirth G, Hacker BR, Massonne H-J (2011) Diapirs as the source of the sediment signature in arc lavas. Nat Geosci 4(9):641-646, doi: 10.1038/ngeo1214

Berner RA (1999) A new look at the long-term carbon cycle. GSA Today 9(11):1-6

Biellmann C, Gillet P, Guyot F, Peyronneau J, Reynard B (1993) Experimental evidence for carbonate stability in the Earth's lower mantle. Earth Planet Sci Lett 118:31-41

Blank JG, Brooker RA (1994) Experimental studies of carbon dioxide in silicate melts: solubility, speciation, and stable carbon isotope behavior. Rev Mineral 30:157-186

Blundy J, Cashman KV, Rust A, Witham F (2010) A case for CO_2-rich arc magmas. Earth Planet Sci Lett 290(3-4):289-301, doi: 10.1016/j.epsl.2009.12.013

Blundy JD, Dalton J (2000) Experimental comparison of trace element partitioning between clinopyroxene and melt in carbonate and silicate systems, and implications for mantle metasomatism. Contrib Mineral Petrol 139:356-371

Brooker RA, Kohn SC, Holloway JR, McMillan PF (2001) Structural controls on the solubility of CO_2 in silicate melts Part II: IR characteristics of carbonate groups in silicate glasses. Chem Geol 174:241-254

Brown JM, Shankland TJ (1981) Thermodynamic parameters in the Earth as determined from seismic profiles. Geophys J Int 66(3):579-596

Brown M (2006) Duality of thermal regimes is the distinctive characteristic of plate tectonics since the Neoarchean. Geology 34(11):961-964

Budyko MI (1969) The effect of solar radiation variations on the climate of the Earth. Tellus 21(5):611-619

Buono AS, Dasgupta R, Lee CT-A, Walker D (submitted) Siderophile element partitioning between cohenite and liquid in Fe-Ni-S-C systems and implications for geochemistry of planetary cores and mantles. Geochim Cosmochim Acta

Campbell IH, O'Neill HSC (2012) Evidence against a chondritic Earth. Nature 483(7391):553-558

Caro G (2011) Early silicate earth differentiation. Annu Rev Earth Planet Sci Lett 39(1):31-58

Cartigny P (2005) Stable isotopes and the origin of diamond. Elements 1(2):79-84

Cartigny P, Pineau F, Aubaud C, Javoy M (2008) Towards a consistent mantle carbon flux estimate: Insights from volatile systematics (H_2O/Ce, δD, CO_2/Nb) in the North Atlantic mantle (14° N and 34° N). Earth Planet Sci Lett 265:672-685

Castro A, Gerya TV (2008) Magmatic implications of mantle wedge plumes: Experimental study. Lithos 103(1-2):138-148, doi: 10.1016/j.lithos.2007.09.012

Catling DC, Zahnle KJ, McKay C (2001) Biogenic methane, hydrogen escape, and the irreversible oxidation of early Earth. Science 293(5531):839-843, doi: 10.1126/science.1061976

Chabot NL, Agee CB (2003) Core formation in the Earth and Moon: New experimental constraints from V, Cr, and Mn. Geochim Cosmochim Acta 67:2077-2091

Chabot NL, Campbell AJ, Jones JH, Humayoun M, Vern Lauer HJ (2006) The influence of carbon on trace element partitioning behavior. Geochim Cosmochim Acta 70:1322-1335

Chou C-L (1978) Fractionation of siderophile elements in the Earth's upper mantle. Proc 9th Lunar Planet Sci Conf 1:219-230

Coltice N, Bertrand H, Rey P, Jourdan F, Phillips BR, Ricard Y (2009) Global warming of the mantle beneath continents back to the Archaean. Gond Res 15(3-4):254-266, doi: 10.1016/j.gr.2008.10.001

Coltice N, Simon L, Lecuyer C (2004) Carbon isotope cycle and mantle structure. Geophys Res Lett 31:L05603, doi: 10.1029/2003GL018873

Condie KC (2004) Supercontinents and superplume events: distinguishing signals in the geologic record. Phys Earth Planet Inter 146(1-2):319-332, doi: 10.1016/j.pepi.2003.04.002

Cooper L, Ruscitto DM, Plank T, Wallace P, Syracuse EM, Manning CE (2012) Global variations in H_2O/Ce I: slab surface temperatures beneath volcanic arcs. Geochem Geophys Geosyst Q03024, doi: 10.1029/2011GC003902

Corgne A, Wood BJ, Fei Y (2008) C- and S-rich molten alloy immiscibility and core formation of planetesimals. Geochim. Cosmochim. Acta 72:2409-2416

Currie CA, Beaumont C, Huismans RS (2007) The fate of subducted sediments: A case for backarc intrusion and underplating. Geology 35(12):1111-1114

Dahl TW, Stevenson DJ (2010) Turbulent mixing of metal and silicate during planet accretion — And interpretation of the Hf-W chronometer. Earth Planet Sci Lett 295(1-2):177-186

Dalou C, Koga KT, Hammouda T, Poitrasson F (2009) Trace element partitioning between carbonatitic melts and mantle transition zone minerals: Implications for the source of carbonatites. Geochim Cosmochim Acta 73(1):239-255

Dalton JA, Presnall DC (1998) Carbonatitic melts along the solidus of model lherzolite in the system CaO-MgO-Al_2O_3-SiO_2-CO_2 from 3 to 7 GPa. Contrib Mineral Petrol 131:123-135

Dasgupta R, Buono A, Whelan G, Walker D (2009a) High-pressure melting relations in Fe-C-S systems: implications for formation, evolution, and structure of metallic cores in planetary bodies. Geochim Cosmochim Acta 73:6678-6691, doi: 10.1016/j.gca.2009.08.001

Dasgupta R, Chi H, Shimizu N, Buono A, Walker D (2012) Carbon cycling in shallow magma oceans of terrestrial planets constrained by high P-T experiments. *In:* 43rd Lunar and Planetary Science Conference, Woodlands, Texas, USA. LPI Contribution No 1659, p 1767

Dasgupta R, Chi H, Shimizu N, Buono A, Walker D (2013a) Carbon solution and partitioning between metallic and silicate melts in a shallow magma ocean: implications for the origin and distribution of terrestrial carbon. Geochim Cosmochim Acta 102:191-212, doi: 10.1016/j.gca.2012.10.011

Dasgupta R, Hirschmann MM (2006) Melting in the Earth's deep upper mantle caused by carbon dioxide. Nature 440:659-662

Dasgupta R, Hirschmann MM (2007a) Effect of variable carbonate concentration on the solidus of mantle peridotite. Am Mineral 92:370-379

Dasgupta R, Hirschmann MM (2007b) A modified iterative sandwich method for determination of near-solidus partial melt compositions. II. Application to determination of near-solidus melt compositions of carbonated peridotite. Contrib Mineral Petrol 154:647-661

Dasgupta R, Hirschmann MM (2010) The deep carbon cycle and melting in Earth's interior. Earth Planet Sci Lett 298:1-13, doi: 10.1016/j.epsl.2010.06.039

Dasgupta R, Hirschmann MM, Dellas N (2005) The effect of bulk composition on the solidus of carbonated eclogite from partial melting experiments at 3 GPa. Contrib Mineral Petrol 149:288-305

Dasgupta R, Hirschmann MM, McDonough WF, Spiegelman M, Withers AC (2009b) Trace element partitioning between garnet lherzolite and carbonatite at 6.6 and 8.6 GPa with applications to the geochemistry of the mantle and of mantle-derived melts. Chem Geol 262:57-77, doi: 10.1016/j.chemgeo.2009.02.004

Dasgupta R, Hirschmann MM, Smith ND (2007a) Water follows carbon: CO_2 incites deep silicate melting and dehydration beneath mid-ocean ridges. Geology 35:135-138, doi: 10.1130/G22856A.1

Dasgupta, R, Hirschmann MM, Smith ND (2007b) Partial melting experiments of peridotite + CO_2 at 3 GPa and genesis of alkalic ocean island basalts. J Petrol 48:2093-2124

Dasgupta R, Hirschmann MM, Withers AC (2004) Deep global cycling of carbon constrained by the solidus of anhydrous, carbonated eclogite under upper mantle conditions. Earth Planet Sci Lett 227:73-85

Dasgupta R, Mallik A, Tsuno K, Withers AC, Hirth G, Hirschmann MM (2013b) Carbon-dioxide-rich silicate melt in the Earth's upper mantle. Nature 493:211-215

Dasgupta R, Walker D (2008) Carbon solubility in core melts in a shallow magma ocean environment and distribution of carbon between the Earth's core and the mantle. Geochim Cosmochim Acta 72:4627-4641, doi: 10.1016/j.gca.2008.06.023

Dauphas N, Davis AM, Marty B, Reisberg L (2004) The cosmic molybdenum-ruthenium isotope correlation. Earth Planet Sci Lett 226(3-4):465-475

Dauphas N, Marty B (2002) Inference on the nature and the mass of Earth's late veneer from noble metals and gases. J Geophys Res 107(E12):5129, doi: 10.1029/2001JE001617

Deines P (2002) The carbon isotope geochemistry of mantle xenoliths. Earth Sci Rev 58(3-4):247-278

Dixon JE (1997) Degassing of alkalic basalts. Am Mineral 82:368-378

Dobson DP, Wiedenbeck M (2002) Fe- and C-self-diffusion in liquid Fe_3C to 15 GPa. Geophys Res Lett 29, doi: 10.1029/2002GL015536

Drake MJ (2005) Origin of water in the terrestrial planets. Meteor Planet Sci 40(4):519-527

Drake MJ, Righter K (2002) Determining the composition of the Earth. Nature 416(6876):39-44

Eggler DH (1976) Does CO_2 cause partial melting in the low-velocity layer of the mantle? Geology 4:69-72

Eggler DH (1983) Upper mantle oxidation state: Evidence from olivine-orthopyroxene-ilmenite assemblages. Geophys Res Lett 10(5):365-368

Eggler DH, Baker DR (1982) Reduced volatiles in the system C O H: implications to mantle melting, fluid formation, and diamond genesis. *In*: Advances in Earth and Planetary Sciences. Vol 12. Akimoto S-I, Manghnani MH (eds), p 237-250

Eggler DH, Rosenhauer M (1978) Carbon dioxide in silicate melts: II. Solubilities of CO_2 and H_2O in $CaMgSi_2O_6$ (diopside) liquids and vapors at pressures to 40 kb. Am J Sci 278(1):64-94

Elkins-Tanton LT (2008) Linked magma ocean solidification and atmospheric growth for Earth and Mars. Earth Planet Sci Lett 271(1-4):181-191

Elkins-Tanton LT (2012) Magma oceans in the inner solar system. Annu Rev Earth Planet Sci 40(1):113-139, doi: 10.1146/annurev-earth-042711-105503

Falloon TJ, Green DH (1989) The solidus of carbonated, fertile peridotite. Earth Planet Sci Lett 94:364-370

Feulner G (2012) The faint young Sun problem. Rev Geophys 50(2):364-370, doi: 10.1016/0012-821X(89)90153-2

Foley SF (2008) Rejuvenation and erosion of the cratonic lithosphere. Nat Geosci 1:503-510

Frezzotti ML, Selverstone J, Sharp ZD, Compagnoni R (2011) Carbonate dissolution during subduction revealed by diamond-bearing rocks from the Alps. Nat Geosci 4(10):703-706

Frost DJ, Liebske C, Langenhorst F, McCammon CA, Tronnes RG, Rubie DC (2004) Experimental evidence for the existence of iron-rich metal in the Earth's lower mantle. Nature 428:409-412

Frost DJ, McCammon CA (2008) The Redox State of Earth's Mantle. Annual Rev Earth Planet Sci 36(1):389-420

Genda H, Abe Y (2003) Survival of a proto-atmosphere through the stage of giant impacts: the mechanical aspects. Icarus 164(1):149-162

Genda H, Abe Y (2005) Enhanced atmospheric loss on protoplanets at the giant impact phase in the presence of oceans. Nature 433(7028):842-844

Gerbode C, Dasgupta R (2010) Carbonate-fluxed melting of MORB-like pyroxenite at 2.9 GPa and genesis of HIMU ocean island basalts. J Petrol 51(10):2067-2088

Gerya TV, Yuen DA (2003) Rayleigh-Taylor instabilities from hydration and melting propel 'cold plumes' at subduction zones. Earth Planet Sci Lett 212(1-2):47-62

Ghosh S, Ohtani E, Litasov KD, Terasaki H (2009) Solidus of carbonated peridotite from 10 to 20 GPa and origin of magnesiocarbonatite melt in the Earth's deep mantle. Chem Geol 262:17-28, doi: 10.1016/j.chemgeo.2008.12.030

Golabek GJ, Schmeling H, Tackley PJ (2008) Earth's core formation aided by flow channelling instabilities induced by iron diapirs. Earth Planet Sci Lett 271(1-4):24-33

Goldberg D, Belton G (1974) The diffusion of carbon in iron-carbon alloys at 1560 °C. Metallurg Mat Trans B 5(7):1643-1648

Gorman PJ, Kerrick DM, Connolly JAD (2006) Modeling open system metamorphic decarbonation of subducting slabs. Geochem Geophys Geosyst 7:Q04007, doi: 10.1029/2005GC001125

Gough DO (1981) Solar interior structure and luminosity variations. Sol Phys 74(1):21-34

Grassi D, Schmidt MW, Günther D (2012) Element partitioning during carbonated pelite melting at 8, 13 and 22 GPa and the sediment signature in the EM mantle components. Earth Planet Sci Lett 327-328(0):84-96

Gudfinnsson G, Presnall DC (2005) Continuous gradations among primary carbonatitic, kimberlitic, melilititic, basaltic, picritic, and komatiitic melts in equilibrium with garnet lherzolite at 3-8 GPa. J Petrol 46:1645-1659

Gudmundsson G, Wood BJ (1995) Experimental tests of garnet peridotite oxygen barometry. Contrib Mineral Petrol 119:56-67

Halliday AN (2004) Mixing, volatile loss and compositional change during impact-driven accretion of the Earth. Nature 427(6974):505-509

Halliday AN (2008) A young Moon-forming giant impact at 70-110 million years accompanied by late-stage mixing, core formation and degassing of the Earth. Phil Trans Royal Soc 366(1883):4163-4181

Hayden LA, Van Orman JA, McDonough WF, Ash RD, Goodrich CA (2011) Trace element partitioning in the Fe-S-C system and its implications for planetary differentiation and the thermal history of ureilites. Geochim Cosmochim Acta 75(21):6570-6583

Hayes JF, Waldbauer JR (2006) The carbon cycle and associated redox processes through time. Phil Trans Royal Soc London B361:931-950

Herzberg C, Asimow PD (2008) Petrology of some oceanic island basalts: PRIMELT2.XLS software for primary magma calculation. Geochem Geophys Geosys 9:Q09001, doi: 10.1029/2008GC002057

Herzberg C, Asimow PD, Arndt N, Niu Y, Lesher CM, Fitton JG, Cheadle MJ, Saunders AD (2007) Temperatures in ambient mantle and plumes: Constraints from basalts, picrites, and komatiites. Geochem Geophys Geosyst 8:Q02006, doi: 10.1029/2006GC001390

Herzberg C, Condie K, Korenaga J (2010) Thermal history of the Earth and its petrological expression. Earth Planet Sci Lett 292(1-2):79-88

Hillgren VJ, Gessmann CK, Li J (2000) An experimental perspective on the light element in Earth's core. *In*: Origin of the Earth and Moon. Canup RM, Righter K (eds) The University of Arizona Press, Tucson, p 245-263

Hirschmann MM (2000) The mantle solidus: experimental constraints and the effect of peridotite composition. Geochem Geophys Geosys 1:2000GC000070

Hirschmann MM (2010) Partial melt in the oceanic low velocity zone. Phys Earth Planet Inter 179(1-2):60-71

Hirschmann MM (2012) Magma ocean influence on early atmosphere mass and composition. Earth Planet Sci Lett 341-344(0):48-57

Hirschmann MM, Dasgupta R (2009) The H/C ratios of Earth's near-surface and deep reservoirs, and consequences for deep Earth volatile cycles. Chem Geol 262:4-16, doi: 10.1016/j.chemgeo.2009.02.008

Hirschmann MM, Withers AC (2008) Ventilation of CO_2 from a reduced mantle and consequences for the early Martian greenhouse. Earth Planet Sci Lett 270(1-2):147-155

Holloway JR, Jakobsson S (1986) Volatile Solubilities in Magmas: Transport of Volatiles from Mantles to Planet Surfaces. J Geophys Res 91(B4):505-508, doi: 10.1029/JB091iB04p0D505

Holloway JR, Pan V, Gudmundsson G (1992) High-pressure fluid-absent melting experiments in the presence of graphite; oxygen fugacity, ferric/ferrous ratio and dissolved CO_2. Eur J Mineral 4(1):105-114

Holzheid A, Sylvester P, O'Neill HSC, Rubie DC, Palme H (2000) Evidence for a late chondritic veneer in the Earth's mantle from high-pressure partitioning of palladium and platinum. Nature 406(6794):396-399

Hopkins M, Harrison TM, Manning CE (2008) Low heat flow inferred from >4 Gyr zircons suggests Hadean plate boundary interactions. Nature 456(7221):493-496

Hopkins MD, Harrison TM, Manning CE (2010) Constraints on Hadean geodynamics from mineral inclusions in >4 Ga zircons. Earth Planet Sci Lett 298(3-4):367-376

Iacono Marziano G, Gaillard F, Pichavant M (2008) Limestone assimilation by basaltic magmas: an experimental re-assessment and application to Italian volcanoes. Contrib Mineral Petrol 155(6):719-738

Iacono-Marziano G, Gaillard F, Scaillet B, Pichavant M, Chiodini G (2009) Role of non-mantle CO_2 in the dynamics of volcano degassing: The Mount Vesuvius example. Geology 37(4):319-322

Ita J, Stixrude L (1992) Petrology, elasticity, and composition of the mantle transition zone. J Geophys Res 97:6849-6866

Jacob DE, Kronz A, Viljoen KS (2004) Cohenite, native iron and troilite inclusions in garnets from polycrystalline diamond aggregates. Contrib Mineral Petrol 146:566-576

Jakobsson S, Holloway JR (1986) Crystal-liquid experiments in the presence of a C-O-H fluid buffered by graphite + iron + wustite: Experimental method and near-liquidus relations in basanite. J Volcan Geotherm Res 29(1-4):265-291

Jarrard RD (2003) Subduction fluxes of water, carbon dioxide, chlorine, and potassium. Geochem Geophys Geosyst 4:8905, doi: 10.1029/2002GC000392

Javoy M, Kaminski E, Guyot F, Andrault D, Sanloup C, Moreira M, Labrosse S, Jambon A, Agrinier P, Davaille A, Jaupart C (2010) The chemical composition of the Earth: Enstatite chondrite models. Earth Planet Sci Lett 293(3-4):259-268

Jones JH, Drake MJ (1986) Geochemical constraints on core formation in the Earth. Nature 322(6076):221-228

Jugo PJ, Wilke M, Botcharnikov RE (2010) Sulfur K-edge XANES analysis of natural and synthetic basaltic glasses: Implications for S speciation and S content as function of oxygen fugacity. Geochim Cosmochim Acta 74:5926-5938

Kadik A, Pineau F, Litvin Y, Jendrzejewski N, Martinez I, Javoy M (2004) Formation of carbon and hydrogen species in magmas at low oxygen fugacity. J Petrol 45:1297-1310

Kadik AA, Kurovskaya NA, Ignat'ev YA, Kononkova NN, Koltashev VV, Plotnichenko VG (2011) Influence of Oxygen Fugacity on the Solubility of Nitrogen, Carbon, and Hydrogen in $FeO-Na_2O-SiO_2-Al_2O_3$ Melts in Equilibrium with Metallic Iron at 1.5 GPa and 1400°C. Geochem Int 49:429-438

Kadik AA, Litvin YA, Koltashev VV, Kryukova EB, Plotnichenko VG (2006) Solubility of hydrogen and carbon in reduced magmas of the early Earth's mantle. Geochem Int 44:33-47

Kaminsky FV, Wirth R (2011) Iron carbide inclusions in lower-mantle diamond from Juina, Brazil. Can Mineral 49(2):555-572

Kasting J (1993) Earth's early atmosphere. Science 259(5097):920-926

Kasting JF, Catling D (2003) Evolution of a habitable planet. Ann Rev Astron Astrophys 41(1):429-463

Kendall JD, Melosh HJ (2012) Fate of iron cores during planetesimal impacts. *In:* 43rd Lunar and Planetary Science Conference, Woodlands, Texas, USA. LPI Contribution No 1659, p 2699

Keppler H, Wiedenbeck M, Shcheka SS (2003) Carbon solubility in olivine and the mode of carbon storage in the Earth's mantle. Nature 424:414-416

Kerrick DM (2001) Present and past nonanthropogenic CO_2 degassing from the solid earth. Rev Geophys 39(4):565-585

Kerrick DM, Connolly JAD (1998) Subduction of ophicarbonates and recycling of CO_2 and H_2O. Geology 26(4):375-378

Kerrick DM, Connolly JAD (2001) Metamorphic devolatilization of subducted oceanic metabasalts: implications for seismicity, arc magmatism and volatile recycling. Earth Planet Sci Lett 189:19-29

Kerridge JF (1985) Carbon, hydrogen and nitrogen in carbonaceous chondrites: Abundances and isotopic compositions in bulk samples. Geochim Cosmochim Acta 49(8):1707-1714

Kirschivink JL (1992) Late Proterozoic low-latitude global glaciation: the snowball Earth. *In*: The Proterozoic Biosphere: A Multidisciplinary Study. Schopf JW, Klein C (eds) Cambridge University Press, p 51-52

Kiseeva ES, Yaxley GM, Hermann J, Litasov KD, Rosenthal A, Kamenetsky VS (2012) An experimental study of carbonated eclogite at 3.5-5.5 GPa—Implications for silicate and carbonate metasomatism in the cratonic mantle. J Petrol 53:727-759, doi: 10.1093/petrology/egr078

Komiya T, Hayashi M, Maruyama S, Yurimoto H (2002) Intermediate-P/T type Archean metamorphism of the Isua supracrustal belt: Implications for secular change of geothermal gradients at subduction zones and for Archean plate tectonics. Am J Sci 302(9):806-826

Kuhn WR, Kasting JF (1983) Effects of increased CO_2 concentrations on surface temperature of the early Earth. Nature 301(5895):53-55

Kuramoto K (1997) Accretion, core formation, H and C evolution of the Earth and Mars. Phys Earth Planet Inter 100:3-20

Kuramoto K, Matsui T (1996) Partitioning of H and C between the mantle and core during the core formation in the Earth: Its implications for the atmospheric evolution and redox state of early mantle. J Geophys Res 101:14909-14932

Lee C-TA, Luffi P, Chin EJ (2011) Building and destroying continental mantle. Ann Rev Earth Planet Sci 39(1):59-90

Lee C-TA, Luffi P, Höink T, Li J, Dasgupta R, Hernlund J (2010) Upside-down differentiation and generation of a 'primordial' lower mantle. Nature 463:930-933, doi: 910.1038/nature08824

Lee C-TA, Shen B, Slotnick B, Liao K, Dickens G, Yokoyama Y, Lenardic A, Dasgupta R, Jellinek M, S. LJ, Schneider T, Tice M (2013) Continent-island arc fluctuations, growth of crustal carbonates, and long-term climate change. Geosphere 9, doi: 10.1130/GES00822.1

Lenardic A, Moresi L, Jellinek AM, O'Neill CJ, Cooper CM, Lee CT (2011) Continents, supercontinents, mantle thermal mixing, and mantle thermal isolation: Theory, numerical simulations, and laboratory experiments. Geochem Geophys Geosyst 12(10):Q10016, doi: 10.1029/2011GC003663

Lesne P, Scaillet B, Pichavant M, Beny J-M (2011) The carbon dioxide solubility in alkali basalts: an experimental study. Contrib Mineral Petrol 162(1):153-168, doi: 10.1007/s00410-010-0585-0

Leung I, Guo W, Friedman I, Gleason J (1990) Natural occurrence of silicon carbide in a diamondiferous kimberlite from Fuxian. Nature 346(6282):352-354

Leung IS (1990) Silicon carbide cluster entrapped in a diamond from Fuxian, China. Am Mineral 75(9-10):1110-1119

Li J, Agee CB (1996) Geochemistry of mantle-core differentiation at high pressure. Nature 381:686-689

Litasov KD, Ohtani E (2009) Solidus and phase relations of carbonated peridotite in the system $CaO-Al_2O_3-MgO-SiO_2-Na_2O-CO_2$ to the lower mantle depths. Phys Earth Planet Int:doi: 10.1016/j.pepi.2009.07.008

Lodders K (2003) Solar system abundances and condensation temperatures of the elements. Astrophys J 591:1220-1247, doi: 10.1086/375492

Lodders K (2010) Solar system abundances of the elements. *In*: Principles and Perspectives in Cosmochemistry: Lecture Notes of the Kodai School on 'Synthesis of Elements in Stars'. Vol. Goswami A, Reddy BE (eds) Springer-Verlag, Berlin Heidelberg, p 379-417

Lord OT, Walter MJ, Dasgupta R, Walker D, Clark SM (2009) Melting in the Fe-C system to 70 GPa. Earth Planet Sci Lett 284:157-167

Luth RW (1993) Diamonds, eclogites, and oxidation state of the Earth's mantle. Science 261:66-68

Luth RW (1999) Carbon and carbonates in the mantle. *In*: Mantle Petrology: Field Observations and High Pressure Experimentation: A Tribute to Francis R. (Joe) Boyd. Vol 6. Fei Y, Bertka, C. M., Mysen, B. O. (ed) The Geochemical Society, p 297-316

Mann U, Frost DJ, Rubie DC (2008) The wetting ability of Si-bearing liquid Fe-alloys in a solid silicate matrix—percolation during core formation under reducing conditions? Phys Earth Planet Inter 167(1-2):1-7

Marty B (2012) The origins and concentrations of water, carbon, nitrogen and noble gases on Earth. Earth Planet Sci Lett 313-314(0):56-66

Marty B, Alexander CMO'D, Raymond SN (2013) Primordial origins of Earth's carbon. Rev Mineral Geochem 75:149-181

Marty B, Jambon A (1987) $C/^3He$ in volatile fluxes from the solid Earth: implications for carbon geodynamics. Earth Planet Sci Lett 83:16-26

Marty B, Tolstikhin IN (1998) CO_2 fluxes from mid-ocean ridges, arcs and plumes. Chem Geol 145:233-248

McCammon CA (2005) Mantle oxidation state and oxygen fugacity: constraints on mantle chemistry, structure, and dynamics. *In*: Earth's Deep Mantle: Structure, Composition, and Evolution. Vol 160. van der Hilst RD, Bass JD, Matas J, Trampert J (eds) American Geophysical Union, Washington D. C., p 221-242

McCammon CA, Kopylova MG (2004) A redox profile of the Slave mantle and oxygen fugacity control in the cratonic mantle. Contrib Mineral Petrol 148:55-68

McDonough WF (2003) Compositional model for the Earth's core. *In*: The Mantle and Core. Vol 2. Carlson RW (ed) Elsevier-Pergamon, Oxford, p 547-568

McDonough WF, Sun S-s (1995) The composition of the Earth. Chem Geol 120:223-253

McKenzie D, Jackson J, Priestley K (2005) Thermal structure of oceanic and continental lithosphere. Earth Planet Sci Lett 233:337-349

Minarik WG, Ryerson FJ, Watson EB (1996) Textural entrapment of core-forming melts. Science 272(5261):530-533

Mints MV, Belousova EA, Konilov AN, Natapov LM, Shchipansky AA, Griffin WL, O'Reilly SY, Dokukina KA, Kaulina TV (2010) Mesoarchean subduction processes: 2.87 Ga eclogites from the Kola Peninsula, Russia. Geology 38(8):739-742

Molina JF, Poli S (2000) Carbonate stability and fluid composition in subducted oceanic crust: an experimental study on H_2O-CO_2-bearing basalts. Earth Planet Sci Lett 176:295-310

Möller A, Appel P, Mezger K, Schenk V (1995) Evidence for a 2 Ga subduction zone: Eclogites in the Usagaran belt of Tanzania. Geology 23(12):1067-1070

Mookherjee M, Nakajima Y, Steinle-Neumann G, Glazyrin K, Wu X, Dubrovinsky L, McCammon C, Chumakov A (2011) High-pressure behavior of iron carbide (Fe_7C_3) at inner core conditions. J Geophys Res 116(B4):B04201

Moore CB, Lewis CF (1967) Total carbon content of ordinary chondrites. J Geophys Res 72(24):6289-6292

Morbidelli A, Chambers J, Lunine JI, Petit JM, Robert F, Valsecchi GB, Cyr KE (2000) Source regions and timescales for the delivery of water to the Earth. Meteor Planet Sci 35(6):1309-1320

Morbidelli A, Lunine JI, O'Brien DP, Raymond SN, Walsh KJ (2012) Building terrestrial planets. Ann Rev Earth Planet Sci 40(1):251-275

Morgan JW, Walker RJ, Brandon AD, Horan MF (2001) Siderophile elements in Earth's upper mantle and lunar breccias: Data synthesis suggests manifestations of the same late influx. Meteor Planet Sci 36(9):1257-1275

Morizet Y, Brooker RA, Kohn SC (2002) CO_2 in haplo-phonolite melt: solubility, speciation and carbonate complexation. Geochim Cosmochim Acta 66(10):1809-1820

Morizet Y, Paris M, Gaillard F, Scaillet B (2010) C-O-H fluid solubility in haplobasalt under reducing conditions: An experimental study. Chem Geol 279(1-2):1-16

Moyen J-F, van Hunen J (2012) Short-term episodicity of Archaean plate tectonics. Geology doi: 10.1130/G32894.32891

Moyen J-Fo, Stevens G, Kisters A (2006) Record of mid-Archaean subduction from metamorphism in the Barberton terrain, South Africa. Nature 442(7102):559-562

Mysen BO (1991) Volatiles in magmatic liquids. *In*: Physical Chemistry of Magma. Advances in Physical Geochemistry, Vol. 9. Perchuk LL, Kushiro I (eds) Cambridge University Press, New York, p 435-476

Mysen BO, Fogel ML, Morrill PL, Cody GD (2009) Solution behavior of reduced COH volatiles in silicate melts at high pressure and temperature. Geochim Cosmochim Acta 73(6):1696-1710

Mysen BO, Kumamoto K, Cody GD, Fogel ML (2011) Solubility and solution mechanisms of C-O-H volatiles in silicate melt with variable redox conditions and melt composition at upper mantle temperatures and pressures. Geochim Cosmochim Acta 75(20):6183-6199

Mysen BO, Yamashita S (2010) Speciation of reduced C-O-H volatiles in coexisting fluids and silicate melts determined in-situ to ~1.4 GPa and 800 °C. Geochim Cosmochim Acta 74(15):4577-4588

Nakajima T, Maruyama S, Uchiumi S, Liou JG, Wang X, Xiao X, Graham SA (1990) Evidence for late Proterozoic subduction from 700-Myr-old blueschists in China. Nature 346(6281):263-265

Nakajima Y, Takahashi E, Toshihiro S, Funakoshi K (2009) "Carbon in the core" revisited. Phys Earth Planet Inter 174:202-211, doi: 10.1016/j.pepi.2008.05.014

Nakamura K, Kato Y (2004) Carbonatization of oceanic crust by seafloor hydrothermal activity and its significance as a CO_2 sink in the Early Archean. Geochim Cosmochim Acta 68:4595-4618

Newsom HE, Sims KWW (1991) Core Formation During Early Accretion of the Earth. Science 252(5008):926-933

Ni H, Keppler H (2013) Carbon in silicate melts. Rev Mineral Geochem 75:251-287

Oganov AR, Hemley RJ, Hazen RM, Jones AP (2013) Structure, bonding, and mineralogy of carbon at extreme conditions. Rev Mineral Geochem 75:47-77

Ohtani H, Nishizawa T (1986) Calculation of Fe-C-S ternary phase diagram. Trans ISIJ 26:655-663

Okuchi T (1997) Hydrogen partitioning into molten iron at high pressure: implications for Earth's core. Science 278:1781-1784

Okuchi T (1998) The melting temperature of iron hydride at high pressures and its implications for the temperature of the Earth's core. J Phys Condens Matter 10:11595-11598

O'Neill C, Lenardic A, Moresi L, Torsvik TH, Lee CTA (2007) Episodic Precambrian subduction. Earth Planet Sci Lett 262(3-4):552-562

Owen T, Bar-Nun A (1995) Comets, impacts, and atmospheres. Icarus 116(2):215-226

Owen T, Cess RD, Ramanathan V (1979) Enhanced CO_2 greenhouse to compensate for reduced solar luminosity on early Earth. Nature 277(5698):640-642

Pawley AR, Holloway JR, McMillan PF (1992) The effect of oxygen fugacity on the solubility of carbon-oxygen fluids in basaltic melt. Earth Planet Sci Lett 110(1-4):213-225

Pineau F, Shilobreeva S, Hekinian R, Bidiau D, Javoy M (2004) Deep-sea explosive activity on the Mid-Atlantic Ridge near 34° 50′ N: a stable isotope (C, H, O) study. Chem Geol 211:159-175

Plank T, Langmuir CH (1998) The geochemical composition of subducting sediment and its consequences for the crust and mantle. Chem Geol 145:325-394

Poirier J-P (1994) Light elements in the Earth's outer core: a critical review. Phys Earth Planet Inter 85:319-337

Ranero CR, Phipps Morgan J, McIntosh K, Reichert C (2003) Bending-related faulting and mantle serpentinization at the Middle America trench. Nature 425(6956):367-373

Raymond SN, Quinn T, Lunine JI (2004) Making other earths: dynamical simulations of terrestrial planet formation and water delivery. Icarus 168(1):1-17

Raymond SN, Quinn T, Lunine JI (2006) High-resolution simulations of the final assembly of Earth-like planets. 1. Terrestrial accretion and dynamics. Icarus 183(2):265-282

Raymond SN, Quinn T, Lunine JI (2007) High-resolution simulations of the final assembly of Earth-like planets. 2. Water delivery and planetary habitability. Astrobiology 7:66-84

Reymer A, Schubert G (1984) Phanerozoic addition rates to the continental crust and crustal growth. Tectonics 3(1):63-77, doi: 10.1029/TC003i001p00063

Righter K (2011) Prediction of metal-silicate partition coefficients for siderophile elements: An update and assessment of PT conditions for metal-silicate equilibrium during accretion of the Earth. Earth Planet Sci Lett 304(1-2):158-167

Rohrbach A, Ballhaus C, Golla-Schindler U, Ulmer P, Kamenetsky VS, Kuzmin DV (2007) Metal saturation in the upper mantle. Nature 449:456-458

Rohrbach A, Ballhaus C, Ulmer P, Golla-Schindler U, Schonbohm D (2011) Experimental evidence for a reduced metal-saturated upper mantle. J Petrol 52(4):717-731

Rohrbach A, Schmidt MW (2011) Redox freezing and melting in the Earth's deep mantle resulting from carbon-iron redox coupling. Nature 472(7342):209-212

Rubie DC, Frost DJ, Mann U, Asahara Y, Nimmo F, Tsuno K, Kegler P, Holzheid A, Palme H (2011) Heterogeneous accretion, composition and core-mantle differentiation of the Earth. Earth Planet Sci Lett 301(1-2):31-42

Saal AE, Hauri E, Langmuir CH, Perfit MR (2002) Vapour undersaturation in primitive mid-ocean-ridge basalt and the volatile content of Earth's upper mantle. Nature 419:451-455

Sagan C, Mullen G (1972) Earth and Mars: Evolution of atmospheres and surface temperatures. Science 177(4043):52-56

Saha L, Hofmann A, Xie H, Hegner E, Wilson A, Wan Y, Liu D, Kröner A (2010) Zircon ages and metamorphic evolution of the Archean Assegaai-De Kraalen granitoid-greenstone terrain, southeastern Kaapvaal Craton. Am J Sci 310(10):1384-1420

Sano Y, Williams SN (1996) Fluxes of mantle and subducted carbon along convergent plate boundaries. Geophys Res Lett 23:2749-2752, doi: 10.1029/96gl02260

Satish-Kumar M, So H, Yoshino T, Kato M, Hiroi Y (2011) Experimental determination of carbon isotope fractionation between iron carbide melt and carbon: ^{12}C-enriched carbon in the Earth's core? Earth Planet Sci Lett 310(3-4):340-348

Schulze DJ, Valley JW, Viljoen KS, Stiefenhofer J, Spicuzza M (1997) Carbon isotope composition of graphite in mantle eclogites. J Geol 105(3):379-386

Shannon MC, Agee CB (1996) High pressure constraints on percolative core formation. Geophys Res Lett 23(20):2717-2720

Sharp WE (1966) Pyrrhotite: a common inclusion in South African diamonds. Nature 211(5047):402-403

Shcheka SS, Wiedenbeck M, Frost DJ, Keppler H (2006) Carbon solubility in mantle minerals. Earth Planet Sci Lett 245:730-742

Shibuya T, Tahata M, Kitajima K, Ueno Y, Komiya T, Yamamoto S, Igisu M, Terabayashi M, Sawaki Y, Takai K, Yoshida N, Maruyama S (2012) Depth variation of carbon and oxygen isotopes of calcites in Archean altered upperoceanic crust: Implications for the CO_2 flux from ocean to oceanic crust in the Archean. Earth Planet Sci Lett 321-322(0):64-73

Shirey SB, Richardson SH (2011) Start of the Wilson cycle at 3 ga shown by diamonds from subcontinental mantle. Science 333(6041):434-436

Shushkanova A, Litvin Y (2008) Diamond formation in sulfide pyrrhotite-carbon melts: Experiments at 6.0-7.1 GPa and application to natural conditions. Geochem Int 46(1):37-47

Siebert J, Corgne A, Ryerson FJ (2011) Systematics of metal-silicate partitioning for many siderophile elements applied to Earth's core formation. Geochim Cosmochim Acta 75(6):1451-1489

Sizova E, Gerya T, Brown M, Perchuk LL (2010) Subduction styles in the Precambrian: Insight from numerical experiments. Lithos 116(3-4):209-229

Sleep NH, Zahnle K (2001) Carbon dioxide cycling and implications for climate on ancient earth. J Geophys Res 106:1373-1399

Stachel T, Brey GP, Harris JW (2005) Inclusions in sublithospheric diamonds: glimpses of deep Earth. Elements 1(2):73-78

Stagno V, Frost DJ (2010) Carbon speciation in the asthenosphere: Experimental measurements of the redox conditions at which carbonate-bearing melts coexist with graphite or diamond in peridotite assemblages. Earth Planet Sci Lett 300(1-2):72-84

Stagno V, Tange Y, Miyajima N, McCammon CA, Irifune T, Frost DJ (2011) The stability of magnesite in the transition zone and the lower mantle as function of oxygen fugacity. Geophys Res Lett 38(19):L19309

Syracuse EM, Abers GA (2006) Global compilation of variations in slab depth beneath arc volcanoes and implications. Geochem Geophys Geosyst 7:Q05017, doi: 10.1029/2005GC001045

Syracuse EM, van Keken PE, Abers GA (2010) The global range of subduction zone thermal models. Phys Earth Planet Inter 183:73-90, doi: 10.1016/j.pepi.2010.02.004

Terasaki H, Frost DJ, Rubie DC, Langenhorst F (2007) Interconnectivity of Fe-O-S liquid in polycrystalline silicate perovskite at lower mantle conditions. Phys Earth Planet Inter 161(3-4):170-176

Terasaki H, Frost DJ, Rubie DC, Langenhorst F (2008) Percolative core formation in planetesimals. Earth Planet Sci Lett 273(1-2):132-137

Terasaki H, Ohtani E, Sakai T, Kamada S, Asanuma H, Shibazaki Y, Hirao N, Sata N, Ohishi Y, Sakamaki T, Suzuki A, Funakoshi K-i (2012) Stability of Fe-Ni hydride after the reaction between Fe-Ni alloy and hydrous phase (δ-AlOOH) up to 1.2 Mbar: Possibility of H contribution to the core density deficit. Phys Earth Planet Inter 194-195(0):18-24

Terasaki H, Shibazaki Y, Sakamaki T, Tateyama R, Ohtani E, Funakoshi K-i, Higo Y (2011) Hydrogenation of FeSi under high pressure. Am Mineral 96(1):93-99

Thibault Y, Holloway JR (1994) Solubility of CO_2 in a Ca-rich leucitite: effects of pressure, temperature, and oxygen fugacity. Contrib Mineral Petrol 116:216-224

Thomsen TB, Schmidt MW (2008) Melting of carbonaceous pelites at 2.5-5.0 GPa, silicate-carbonatitie liquid immiscibility, and potassium-carbon metasomatism of the mantle. Earth Planet Sci Lett 267:17-31

Trail D, Watson EB, Tailby ND (2011) The oxidation state of Hadean magmas and implications for early Earth's atmosphere. Nature 480(7375):79-82

Trull T, Nadeau S, Pineau F, Polve M, Javoy M (1993) C-He systematics in hotspot xenoliths: implications for mantle carbon contents and carbon recycling. Earth Planet Sci Lett 118:43-64

Tsuno K, Dasgupta R (2011) Melting phase relation of nominally anhydrous, carbonated pelitic-eclogite at 2.5-3.0 GPa and deep cycling of sedimentary carbon. Contrib Mineral Petrol 161:743-763

Tsuno K, Dasgupta R (2012) The effect of carbonates on near-solidus melting of pelite at 3 GPa: Relative efficiency of H_2O and CO_2 subduction. Earth Planet Sci Lett 319-320(0):185-196

Tsuno K, Dasgupta R, Danielson L, Righter K (2012) Flux of carbonate melt from deeply subducted pelitic sediments - geophysical and geochemical implications for the source of Central American volcanic arc. Geophys Res Lett 37:L16307, doi: 10.1029/2012GL052606

Tsymbulov LB, Tsmekhman LS (2001) Solubility of carbon in sulfide melts of the system Fe-Ni-S. Russ J Appl Chem 74:925-929

van Keken PE, Kiefer B, Peacock SM (2002) High-resolution models of subduction zones: Implications for mineral dehydration reactions and the transport of water into the deep mantle. Geochem Geophys Geosyst 3:1056, doi: 10.1029/2001GC000256

Walker D, Dasgupta R, Li J, Buono A (accepted) Nonstoichiometry and growth of some Fe-carbides. Contrib Mineral Petrol

Walker JCG, Hays PB, Kasting JF (1981) A negative feedback mechanism for the long-term stabilization of Earth's surface temperature. J Geophys Res 86(C10):9776-9782

Walker RJ, Horan MF, Morgan JW, Becker H, Grossman JN, Rubin AE (2002) Comparative [187]Re-[187]Os systematics of chondrites: Implications regarding early solar system processes. Geochim Cosmochim Acta 66(23):4187-4201

Wallace ME, Green DH (1988) An experimental determination of primary carbonatite magma composition. Nature 335:343-346

Walter MJ, Kohn SC, Araujo D, Bulanova GP, Smith CB, Gaillou E, Wang J, Steele A, Shirey SB (2011) Deep mantle cycling of oceanic crust: evidence from diamonds and their mineral inclusions. Science 334(6052):54-57

Wang C, Hirama J, Nagasaka T, Ban-Ya S (1991) Phase equilibria of liquid Fe-S-C ternary system. ISIJ Int 31:1292-1299

Wänke H, Dreibus G (1988) Chemical composition and accretion history of terrestrial planets. Phil Trans R Soc Lond 325:545-557

Warren PH (2011) Stable-isotopic anomalies and the accretionary assemblage of the Earth and Mars: A subordinate role for carbonaceous chondrites. Earth Planet Sci Lett 311(1-2):93-100

Wetzel DT, Jacobsen SD, Rutherford MJ, Hauri EH, Saal AE (2012) The solubility and speciation of carbon in lunar picritic magmas. *In:* 43rd Lunar and Planetary Science Conference, Woodlands, Texas, USA. LPI Contribution No. 1659, p 1535

Wood BJ (1993) Carbon in the core. Earth Planet Sci Lett 117:593-607

Wood BJ (1995) Storage and recycling of H_2O and CO_2 in the earth. AIP Conf Proc 341(1):3-21

Wood BJ, Halliday AN (2010) The lead isotopic age of the Earth can be explained by core formation alone. Nature 465(7299):767-770

Wood BJ, Pawley A, Frost DR (1996) Water and carbon in the Earth's mantle. Philos Trans R Soc London 354:1495-1511

Wood BJ, Walter MJ, Wade J (2006) Accretion of the Earth and segregation of its core. Nature 441:825-833

Wood BJ, Li J, Shahar A (2013) Carbon in the core: its influence on the properties of core and mantle. Rev Mineral Geochem 75:231-250

Woodland AB, Koch M (2003) Variation in oxygen fugacity with depth in the upper mantle beneath the Kaapvaal craton, South Africa. Earth Planet Sci Lett 214:295-310

Wyllie PJ (1977) Peridotite-CO_2-H_2O, and carbonatitic liquid in the upper asthenosphere. Nature 266:45-47

Yaxley GM, Berry AJ, Kamenetsky VS, Woodland AB, Golovin AV (2012) An oxygen fugacity profile through the Siberian Craton — Fe K-edge XANES determinations of Fe^{3+}/ΣFe in garnets in peridotite xenoliths from the Udachnaya East kimberlite. Lithos 140-141(0):142-151

Yaxley GM, Brey GP (2004) Phase relations of carbonate-bearing eclogite assemblages from 2.5 to 5.5 GPa: implications for petrogenesis of carbonatites. Contrib Mineral Petrol 146:606-619

Yaxley GM, Green DH (1994) Experimental demonstration of refractory carbonate-bearing eclogite and siliceous melt in the subduction regime. Earth Planet Sci Lett 128:313-325

Yi W, Halliday AN, Alt JC, Lee D-C, Rehkämper M, Garcia MO, Langmuir CH, Su Y (2000) Cadmium, indium, tin, tellurium, and sulfur in oceanic basalts: Implications for chalcophile element fractionation in the Earth. J Geophys Res 105(B8):18927-18948

Zahnle K, Arndt N, Cockell C, Halliday A, Nisbet E, Selsis F, Sleep N (2007) Emergence of a habitable planet. Space Sci Rev 129(1):35-78

Zahnle K, Schaefer L, Fegley B (2010) Earth's Earliest Atmospheres. Cold Spring Harb Perspect Biol 2(10):a004895, doi: 10.1101/cshperspect.a004895

Zahnle KJ (2006) Earth's Earliest Atmosphere. Elements 2(4):217-222

Zhang C, Duan Z (2009) A model for C-O-H fluid in the Earth's mantle. Geochim Cosmochim Acta 73(7):2089-2102

Zhimulev E, Chepurov A, Sinyakova E, Sonin V, Pokhilenko N (2012) Diamond crystallization in the Fe-Co-S-C and Fe-Ni-S-C systems and the role of sulfide-metal melts in the genesis of diamond. Geochem Int 50(3):205-216